



All Theses and Dissertations

2018-03-01

Toward a Production Ready FBJ Process for Joining Dissimilar Combinations of GADP 1180 Steel and AA 7085-T76

Kevin Alexander Shirley
Brigham Young University

Follow this and additional works at: <https://scholarsarchive.byu.edu/etd>

 Part of the [Manufacturing Commons](#)

BYU ScholarsArchive Citation

Shirley, Kevin Alexander, "Toward a Production Ready FBJ Process for Joining Dissimilar Combinations of GADP 1180 Steel and AA 7085-T76" (2018). *All Theses and Dissertations*. 6694.
<https://scholarsarchive.byu.edu/etd/6694>

This Thesis is brought to you for free and open access by BYU ScholarsArchive. It has been accepted for inclusion in All Theses and Dissertations by an authorized administrator of BYU ScholarsArchive. For more information, please contact scholarsarchive@byu.edu, ellen_amatangelo@byu.edu.

Toward a Production Ready FBJ Process for Joining Dissimilar
Combinations of GADP 1180 Steel and AA 7085-T76

Kevin Alexander Shirley

A thesis submitted to the faculty of
Brigham Young University
in partial fulfillment of the requirements for the degree of

Master of Science

Mike P. Miles, Chair
Jason M. Weaver
Yuri Hovanski

School of Technology
Brigham Young University

Copyright © 2018 Kevin Alexander Shirley

All Rights Reserved

ABSTRACT

Toward a Production Ready FBJ Process for Joining Dissimilar Combinations of GADP 1180 Steel and AA 7085-T76

Kevin Alexander Shirley
School of Technology, BYU
Master of Science

Friction Bit Joining (FBJ) is a new technology that can be used to join dissimilar materials together. This ability makes it a good candidate for creating light weight structures for the automotive industry by combining lightweight materials such as aluminum to stronger materials like advanced high-strength steels. The automotive industry and many other industries have great interest in reducing structure weight to increase fuel efficiency.

The purpose of this research is to make FBJ of GADP 1180 to AA 7085-T76 a production ready process by (1) better understanding the effects of process parameters, bit design and tool design on joint strength and reliability especially as they relate to different joint configurations; (2) determining if consecutive FBJ joints on a part will be additive in strength; (3) improving surface finish for better coating adhesion so that joints can be made to withstand extended corrosion testing; and (4) determining the failure modes and fatigue life of joint components at high and low load amplitudes.

No universal parameter set for optimizing peak load for T-peel, cross tension, and lap-shear tension configurations were found. Due to the extreme load conditions of T-peel and the smaller margin of safety it is better to optimize for T-peel. However, strength and reliability were still improved across the board. Cutting features and tapered shanks were found to not always be necessary. Removing cutting features from the bit design increased peak weld cycle loads, but a stiffer machine can overcome this. Consecutive FBJ joints on a part are mostly additive in nature. When the weakest joint fails, its load is distributed to the remaining joints and will limit the peak load of the whole part. If all joints are “good” then the peak load will be approximately additive. Most of the stress is localized on the side of the bit opposite of the pulling direction. Failure modes in lap-shear tend to change from weld nugget pullouts in single weld specimens to aluminum material failures in multi-weld specimens. This is because of the added stiffness that additional material and welds provide to resist coupons bending and creating a peeling action. Surface finish was improved by development of a floating carbide cutting system which cut aluminum flash as it was generated around the head of the bit. A new internal drive design provided the ability to drive bits flush with the aluminum top layer if desired with minimal reductions in strength. Flush bits provided benefits in safety, cosmetics, and coating adhesion.

Keywords: FBJ, dissimilar material joining, advanced high-strength steel, aluminum, GADP 1180, automotive manufacturing, aerospace manufacturing, corrosion, flush joints

ACKNOWLEDGEMENTS

I wish to express appreciation to everyone who contributed to and supported these efforts towards the development of friction bit joining research. Dr. Mike Miles was a patient and encouraging mentor offering technical guidance and professional advice. Shane Wood, a fellow masters student on the project, kept the project alive with humor and ingenuity that solved many problems. Many of the employees at the BYU Manufacturing Department machine shop brought fresh perspectives and extra hands that helped push the project over important hurdles.

Oak Ridge National Laboratory and MegaStir offered collaborative technical efforts that helped bring this project to completion. Honda and the Department of Energy provided direction and funding for the research.

TABLE OF CONTENTS

ABSTRACT.....	ii
TABLE OF CONTENTS.....	iv
LIST OF TABLES.....	vi
LIST OF FIGURES.....	vii
1 Introduction.....	1
1.1 Background.....	1
1.2 Problem Statement.....	2
1.3 Research Questions.....	3
1.4 Hypotheses.....	3
1.5 Methodology.....	4
1.5.1 Materials.....	4
1.5.2 Experiments.....	5
1.6 Delimitations and Assumptions.....	6
1.7 Glossary.....	6
2 Literature Review.....	8
2.1 Introduction.....	8
2.2 Need for Lighter Weight Vehicles.....	8
2.3 Joining UHSS to Aluminum.....	9
3 Experimental Design.....	11
3.1 Summary.....	11
3.2 The FBJ Machine.....	12
3.3 The FBJ Process and Phases.....	14
3.4 Failure Modes in Tensile Testing.....	15
3.5 Equipment and Testing.....	16
3.5.1 Equipment.....	16
3.5.2 Lap-Shear Tension.....	17
3.5.3 Cross-Tension.....	18
3.5.4 T-Peel.....	19
3.5.5 Fatigue.....	20
3.5.6 Corrosion.....	20
3.5.7 Automotive Standards for Spot Joint Performance.....	21

4	Research Results and Analysis	22
4.1	Process Improvement	22
4.2	Design of Experiments	27
4.3	Fatigue	36
4.4	Multi-Weld Lap-Shear Tensile Test Samples	40
4.5	Bit and Driver Design	50
4.6	Surface Finish.....	63
4.7	Corrosion.....	71
5	Conclusions and Recommendations	73
5.1	Conclusions	73
5.2	Recommendations	76
	References.....	77

LIST OF TABLES

Table 3-1: Automotive Standards for Spot Joint Performance.....	21
Table 4-1 : Lap-Shear Peak Loads with New Parameters	28
Table 4-2: T-Peel Peak Load with New Parameters.....	28
Table 4-3: DOE Variables	30
Table 4-4: Average Peak Loads for Parameter Meeting All Requirements	36
Table 4-5: High Load Fatigue Results	37
Table 4-6: Medium Load Fatigue Results	37
Table 4-7: Low Load Fatigue Results.....	37
Table 4-8 Multi-Weld Lap-Shear Tensile Test Results	41
Table 4-9: Multi-Weld Lap-Shear Peak Loads at Different Spacings	48
Table 4-10: Lap-shear Peak Loads of Bits with No Cutting Features	52
Table 4-11: T-Peel Peak Loads with Flush FBJ	62

LIST OF FIGURES

Figure 3-1: Prototype FBJ Machine.....	13
Figure 3-2: FBJ Diagram	15
Figure 3-3: Failure Modes	16
Figure 3-4: Method for Gripping Shear Specimens.....	17
Figure 3-5: Lap-Shear Tension Configuration.....	18
Figure 3-6: Cross-Tension Configuration.....	19
Figure 3-7: T-Peel Configuration.....	19
Figure 3-8: Hydraulic Instron for Fatigue Testing.....	20
Figure 4-1: FBJ Machine Z Force vs. Deflection	22
Figure 4-2: FBJ Machine Points of Deflection Measurement	23
Figure 4-3: Pneumatic Clamp Before Installation on the FBJ Machine.....	24
Figure 4-4: Pneumatic Clamp Side View	25
Figure 4-5: Pneumatic Clamp Actuated by Air Piston Underneath the Anvil.....	25
Figure 4-6: DOE FBJ Bit Design.....	30
Figure 4-7: Lap-Shear Tension IPM to Z Depth Relationship in kN	33
Figure 4-8: Cross Tension IPM to Z Depth Relationship	34
Figure 4-9: T-Peel IPM to Z Depth Relationship	35
Figure 4-10: .5-5kN Fatigue Sample Nugget Pullout and AA Material Failure.....	38
Figure 4-11: .5-5kN Fatigue Samples with Nugget Pullout Failure	38
Figure 4-12: .5-5kN Fatigue Sample Weld Nugget Pullout Failure	39
Figure 4-13: .25-2.5kN AA Material Failure Only in All Three Samples.....	39
Figure 4-14: 3 Weld, 40mm Spacing on 120mm Wide Lap-Shear Specimens	40

Figure 4-15: Example of "Good" Welds with Aluminum Only Failure Modes	43
Figure 4-16 "Bad" Weld with One Interfacial Failure and Two AA Failures	44
Figure 4-17 "Bad" Weld Failure Modes	45
Figure 4-18: 2 Weld, 80mm Spacing on 100mm Wide Lap-Shear Specimens	46
Figure 4-19: 2 Weld, 70mm Spacing on 100mm Wide Lap-Shear Specimens	47
Figure 4-20: 2 Weld, 80mm Spacing on 120mm Wide Lap-Shear Specimens	47
Figure 4-21: 2 Weld, 60mm Spacing on 100mm Wide Lap-Shear Specimens	48
Figure 4-22: DIC Results for a Multi-Weld Sample with 3 FBJ Joints.....	49
Figure 4-23: Testing FBJ Cutting Features with CNC Mill	51
Figure 4-24: FBJ with Cap to Cover Aluminum Flash Instead of Removing It.....	51
Figure 4-25: Proof-of-Concept Flush Joints Made with Machine Screws	54
Figure 4-26: Torx Plus Driver Welded to Bit	55
Figure 4-27: Fracture After Removing Welded Driver from the Bit.....	55
Figure 4-28: Bit Head Cracking.....	57
Figure 4-29: Severe Fracture of Bit Head.....	57
Figure 4-30: Severe Fracture of Bit Head.....	57
Figure 4-31: Crack Flowing Aluminum into Drive Feature of Bit.....	58
Figure 4-32: Overall Geometries of Current Flush Bit Design.....	58
Figure 4-33: Drive Features of Current Bit Design	59
Figure 4-34: Isometric View of Flush FBJ	59
Figure 4-35: Unpolished Flush FBJ Cross Section.....	59
Figure 4-36: Flush FBJ Side View.....	60
Figure 4-37: Dies for Pressing Drive Features into Bit Heads	60

Figure 4-38: Severe Smearing of Drive Features During Experiment	61
Figure 4-39: Less Common Stretching of Drive Features	61
Figure 4-40: Polished Cross Section Microscope View of Flush FBJ Joint.....	63
Figure 4-41: Section View of Flash Removal Clamp with Bushing	64
Figure 4-42: Leftover Flash from Driver with Fixed Cutters	65
Figure 4-43: Driver with Three Pegs, Fixed Carbide, and Bit.....	66
Figure 4-44: 4 Peg Driver Assembly	66
Figure 4-45: Aluminum Chip Build Up Due to Uneven Cutter Engagement	67
Figure 4-46: Flush Bit Driver After Several Hundred Welds.....	68
Figure 4-47: Flush Bit Driver Full Side View	68
Figure 4-48: Flush Bit Cutter Assembly.....	69
Figure 4-49: Underside View of Cutter Assembly Mounted in Clamp Block	69
Figure 4-50: Cutter Assemebly with Needle Bearing and Thrust Bearing.....	70
Figure 4-51: Broken Cutter After Bit Jammed In Clamp Block.....	70
Figure 4-52: Full Clamp-Cutter-Driver Assembly	71

1 INTRODUCTION

1.1 Background

New CAFE standards set by the Federal government mandate that automotive manufacturers increase their average MPG for their trucks and cars to at least 54.5 by the year 2025. This is a lofty goal with current technologies and that is why new technologies are needed. There are two approaches to improving fuel economy: increase efficiencies in the engine and drivetrain or reducing the mass of the vehicle. The scope of this research is focused on reducing mass.

Reducing mass, also known as light-weighting, can be accomplished by using materials with higher strength to weight ratios and using less material. However, not all components of a vehicle need to be equally strong. Using mixed-materials, designers can use stronger materials which are usually heavier or more expensive where they are needed and use weaker materials which are usually lighter and cheaper where strength requirements are not as high. Two potential materials of interest to the automotive industry are Ultra High Strength Steel (UHSS) and aluminum.

Despite efforts to use old joining techniques and to develop new ones, few joining technologies show promise in joining these two materials together. Friction welding, diffusion bonding, self-piercing rivets, fusion bonding, friction stir spot welding, adhesive bonding and

friction stir welding each fall short of the desired bond, material, and process characteristics needed. Problems such as brittle intermetallic compounds and insufficient strength prevent these technologies from succeeding. But a new technology has shown promise.

Friction Bit Joining (FBJ) has successfully used a steel, consumable bit which is drilled through an aluminum top layer until the bit rubs on the steel lower layer resulting in a friction induced solid state bond. The head of the bit pinches the aluminum down while the shank of the bit creates a strong metallurgical bond with the steel. The relatively low temperatures and plastic deformation avoids many of the problems encountered by other technologies.

Recent research has shown that FBJ can create welds of satisfactory strength between UHSS and aluminum. Preliminary efforts have been made to establish process parameters, bit designs, and machine configurations that will optimize strength and reliability, but further work is needed to reliably achieve the required strength for the following standard tests: T-peel, static lap shear, cross-tension, fatigue, and corrosion. Issues of excessive aluminum flash and debris still being attached to the joint have prevented full application of corrosion resistant coatings which leads to premature failures in corrosion tests. Another matter of interest is confirming the additive nature of multiple FBJ welds applied in the same sample along with adhesives. In addition, an appropriate production method for the bits still needs to be identified and verified.

When these issues are resolved FBJ will stand as a robust, viable joining method for UHSS and aluminum in a high-volume production environment.

1.2 Problem Statement

The purpose of this research is to further understand the relationship of process parameters, bit design, and machine construction so that strength and reliability can be optimized in a

commercial setting where multiple, consecutive FBJ welds are used with adhesives and corrosion resistant coatings so that neither adhesive or coatings are degraded.

1.3 Research Questions

The questions addressed during this research include the following:

1. Can the reliability and strength of FBJ of GADP 1180 to AA 7085-T76 be optimized in lap-shear, t-peel and cross-tension with adhesives and multiple welds per sample?
2. Is the strength of consecutive FBJ welds parallel to the bonded edge on the same work piece additive regardless of their spacing and whether the welds are made in combination with an adhesive?
3. Are cutting features on FBJ bits beneficial to FBJ of GADP 1180 to AA 7085-T76 as compared to a bit with no cutting features?
4. How does FBJ with bits with a straight shank compare with a bit with a tapered shank?
5. How can surface finish be preserved for future coatings?
6. In a FBJ joint of GADP 1180 to AA 7085-T76, what component will fail first in low load, high cycle fatigue testing and in high load, low cycle fatigue testing?
7. Can FBJ joints of GADP 1180 to AA 7085-T76 be made to withstand corrosion testing if protected by a corrosion inhibiting coating after being joined?

1.4 Hypotheses

1. Machine parameters, bit design and machine design can be optimized through empirical testing for strength and reliability in T-peel, lap shear, and cross tension though each test may require a different combination for optimization.

2. The strength of consecutive FBJ welds parallel to the bonded edge on the same work piece are additive regardless of their spacing and whether the welds are made in combination with an adhesive.
3. Cutting features on FBJ bits are not always beneficial to FBJ of GADP 1180 to AA 7085-T76 as compared to a bit with no cutting features.
4. Surface finish can be improved through machine parameter, bit design and tool design optimization.
5. In a FBJ joint of GA DP 1180 to AA 7085-T76 the aluminum will fail first in low load, high cycle fatigue testing, but the steel will fail first in high load, low cycle fatigue testing.
6. FBJ joints of GADP 1180 to AA 7085-T76 can be made to withstand corrosion testing if protected by a corrosion inhibiting coating after being joined.

1.5 Methodology

1.5.1 Materials

Only 0.8 mm thick GADP1180 and 2 mm thick AA7085 were joined. Material parameters were set by sponsors to assure that results were directly transferable to their needs. All joints were made with the steel layer on bottom and the aluminum layer on top. Coupons for single weld lap shear were 125 mm by 40 mm with a 20 mm overlap. Coupons for multi-weld lap shear were either 120 mm or 100 mm by 125 mm. Coupons for single weld t-peel were 40 mm wide with a 35 mm straight section followed by a 45-degree bend with a 5 mm internal radius and then an 80 mm straight section. Cross tension coupons were 50 mm by 150 mm with a 20 mm holes drilled 25 mm from each end of each coupon.

The FBJ bits were made of 1018 steel which were then heat treated to 40-47 HRC after the bits had been machined and pressed. Bits were produced using a CNC lathe, a die set and 25-ton hydraulic press, and an oven for heat treating.

Joints were made using a prototype FBJ machine designed by MegaStir Technologies. Further modifications to the machine were made by the Precision Machining Lab at Brigham Young University and by members of the FBJ research team.

1.5.2 Experiments

To answer the research questions, a series of experiments were performed that involved destructive testing of FBJ samples. Lap-shear tension, T-peel, and cross-tension samples were pulled to failure with an Instron to determine the peak loads and repeatability of the FBJ process. Specific process parameters were varied to determine their effect on strength and repeatability. These parameters were Z depth, RPM, Z velocity, and dwell time at each stage of the weld cycle. Aside from process parameters, machine, driver and bit design were varied to determine their effects on peak load and repeatability as well as to determine effect on surface finish. Larger multi-weld lap-shear tension samples were created to determine the effects of subsequent welds on joint strengths. Some lap-shear tension samples went through fatigue life testing to determine their fatigue characteristics. A series of lap-shear tension samples were also produced with and without an additional layer of adhesive. These samples will undergo accelerated corrosion testing to determine and improve the corrosion resistance of FBJ joints.

Through statistical analysis, the relationships of process parameters, bit design, machine design, driver design, adhesives, and number and spacing of welds to strength, reliability, fatigue life, and corrosion were determined.

1.6 Delimitations and Assumptions

No other materials besides GADP 1180 and AA7085-T76 were investigated for joining. No other bit materials beside 1018 steel were investigated for bit materials.

1.7 Glossary

AHSS – advanced high-strength steel (steels that yield at 560 MPa or above)

DP – dual phase steel that has a ferrite and martensitic microstructure

GADP1180 – a galvanized high-strength dual-phase steel with an ultimate tensile strength of 1180 MPa

EDM – electronic discharge machining. Two types were used during this work: wire

EDM and plunge EDM.

FBJ – friction bit joining uses a consumable bit to spot join sheet metals by drilling through the top sheet and friction-welding to the bottom sheet.

FSSW – friction stir spot welding is a solid-state welding process that uses a non-consumable tool to stir the metals to be joined together at a point.

GA- protective zinc coating to prevent rust.

HAZ – heat-affected zone is the area within a material that has changed properties due to welding or some other heat intensive processes.

IMC – intermetallic compound is formed when dissimilar metals diffuse together at a weld interface.

ORNL – Oak Ridge National Laboratory

RSW – resistance spot welding is a fusion-welding process that uses electrodes to clamp the sheet metals together and pass a current through them which produces the necessary welding heat.

RPM – revolutions per minute

SPR – self-piercing riveting is a cold process that uses a die set to force a rivet into sheet metal without predrilling a hole.

UTS – ultimate tensile strength

2 LITERATURE REVIEW

2.1 Introduction

Literature specifically on the topic of Friction Bit Joining is sparse because it is a new technology. Most of the literature reviewed was examined to understand the alternative processes for joining dissimilar metals, especially Ultra-High Strength Steel to aluminum and to understand the automotive industry's motivations for light-weighting vehicles.

2.2 Need for Lighter Weight Vehicles

Government regulations known as CAFE standards have mandated that automotive manufacturers increase the average MPG of their vehicles to 54.5 MPG by 2025. Fuel efficiency can be improved by increasing power plant efficiency, increasing power delivery efficiency or by reducing the load carried. Up to 72% of respondents to a survey given to automotive manufacturers responded that light-weighting vehicles is how their companies plan to meet the CAFE standard (Deptula, 2015). Car manufacturers want “to make cars lightweight and crashworthy, while reducing costs and meeting performance mandates” (Schneider, 2017). Many new materials, technologies, products and environmental affects will develop because of light-weighting in the automotive industry (Albrecht, 2013).

Light-weighting can be achieved by eliminating unnecessary material and by substituting in materials with better strength to weight ratios. Composites processes are being developed, but

costs and processing time are currently limiting factors which prevent composites from solving weight problems for all vehicles. Another alternative being pursued is the use of Advanced High Strength Steel (AHSS) (Matlock, 2009) where strength is needed and aluminum is used where it is less important. AHSS's reasonable ductility and formability (Kuziak, 2008) along with high tensile strength make it a candidate for mixed-material body structures (Lai, 2007). Lightweighting of closures (i.e. doors) has the added benefit of multiplying weight losses by the number of that given closure used in the vehicle (Deptula, 2015).

2.3 Joining UHSS to Aluminum

A car body made from just UHSS would not be optimized for weight and a car body made from just aluminum would not be optimized for strength. A combination of UHSS and aluminum is desirable, but joining technologies are limited when it comes to this material combination. Some of the common problems with joining UHSS to aluminum alloys are the difference in flow stress (Abe, 2006) and the fact that the aluminum and UHSS tend to form brittle intermetallic compounds during bonding (Miles, 2009).

Current technologies include Resistance Spot Welding (RSW), Friction Spot Welding (FSW), and Self Piercing Rivets (SPR). RSW requires an additional layer of material for compatibility in the weld. It offers good weld strength but has low energy absorption. When Qie and et al. (Qiu, 2009) resistance spot welded AA5052 (1 mm thick) to austenitic stainless steel SUS304 (1 mm thick) they obtained a lap shear strength of 6.5 kN. A drawback to RSW for UHSS is that it destroys the microstructure in the fusion zone (FZ) and the heat affected zone (HAZ) through microstructure transformations (Pouranvari, 2013).

FSW, which was developed in 1991, maintains a small HAZ, short cycle times and relatively good weld quality by keeping temperatures below the melting temperature of the parent material using friction (Rhodes, 1997). But so far, FSW maxes at 3 kN for peak load in lap shear which is below some requirements.

SPR, a form of cold-forming that has been used for joining dissimilar metals in the past (Groche, 2014), is competitive in strength at 5 kN, but does not bond well with UHSS (Miles, 2010). SPR has been successfully used to bond aluminum to steel sheets with a UTS of up to 590 Mpa, but above that, the rivets are too weak to deform the steel (Abe, 2009). Automotive companies have already indicated interest in using UHSS with a strength of 1180 Mpa, far beyond what SPR is currently capable of.

Friction Bit Joining (FBJ) is a viable alternative with documented peak loads in lap-shear in 1.4 mm DP980 to 1.8 mm AA5754-O coming in around 5 kN (Miles, 2010). Examining FBJ weld microstructures has shown that it can create defect-free joints (Huang, 2009). Previous FBJ research has used similar principles and designs to current research (i.e. a consumable steel friction bit being spun and pushed through an aluminum upper sheet until contact with a steel under sheet which results in frictional heating and a subsequent solid-state bond). Published test results so far have shown that generally harder bits penetrate farther into the steel, fluted bit designs average better peak loads in lap shear, but “flat” designs (without flutes) have greater individual peak loads. Rotational speed of the bit and plunge rate have noticeable effects on bond strength (Miles, 2010). FBJ research has covered cast-iron, carbon fiber, Al 5574, Al 7075, Al 7085, DP980, and DP590 (Miles, 2010, 2013), but not GADP1180. FBJ has so far proven a viable candidate for bonding UHSS to aluminum alloys.

3 EXPERIMENTAL DESIGN

3.1 Summary

Lap-shear joints, cross-tension joints, and T-peel joints were made using a purpose-built Friction Bit Joining machine. Hypotheses were tested, and research questions were answered by performing relevant tests on these joints to identify the relationships of variables of concern to FBJ. A variety of bits were produced for testing using a CNC lathe, hydraulic press, dies, and an oven for heat treating. Instron equipment was used to test mechanical strength of the joints. A digital camera was used to collect images for Digital Image Correlation to confirm stress-patterns in select samples. Visual inspections of samples were also used to collect information. A select set of independent variables were controlled to try to optimize specific dependent variables. Clamp and driver designs were heavily modified as need arose throughout development.

Independent variables:

- Bit geometry
- Weld parameters: clamp force, Z depth, Z velocity, RPM, dwell time
- Number of welds per specimen and spacing
- Presence of adhesives

- Types of adhesives
- Driver and clamp geometry

Dependent variables:

- Peak load
- Failure mode
- Cycles till failure
- Duration of time surviving corrosion test
- Surface finish

3.2 The FBJ Machine

MegaStir Technologies built the Friction Bit Joining machine used for this research. This C-frame based, automatic drill press with a braking device precisely controls RPM (maximum 4000 RPM), federate (IPM), Z-depth and dwell delays in up to four stages. The machine moves to the next stage when the previous stage reaches its depth and dwell time. Stages can be turned off if they are not needed. The machine can also be set to change stages when a certain Z load is detected by a load cell located in the anvil of the machine. However, due to hardware limitations in the PLC, the machine's sample rate cannot exceed 17 Hz. Because whole process takes around two seconds and the pressure spike can exceed 20 kN, 17 Hz is not a fast enough sample rate to precisely control the process.

A collet accepts a 3/8" shank tool. A fixture mounted below the spindle holds specimens in a variety of orientations for the desired test types. Samples were at first clamped down with a pressure bar and two bolts. More consistent and faster pneumatic clamps were eventually designed and implemented to address needs and concerns of tests.

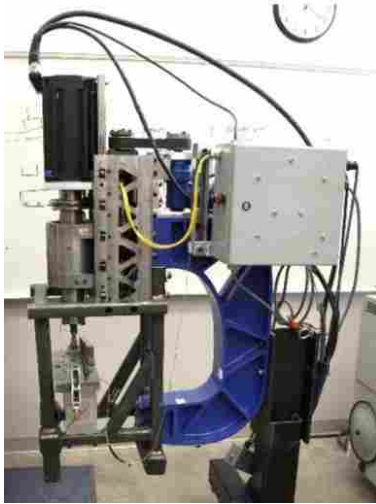


Figure 3-1: Prototype FBJ Machine

A PLC and a laptop work in combination to process RPM, Z velocity, Z depth and dwell time feedback and control the process. Through an HMI on the laptop, these variables can be set for up to four stages. Stages can be controlled per position or load.

The FBJ machine software automatically recorded and stored weld cycle information. It kept a record of the following parameters and assigned it to a weld number:

- Z load
- Z torque
- Z velocity
- RPM
- Weld duration
- Z depth

3.3 The FBJ Process and Phases

The FBJ process consists of three phases. In the first phase, a consumable bit is secured by a driver and spun and lowered into the top layer of material at the RPM and Z velocity set in the first stage of the program. The bit either cuts through the material or pushes through the material via frictional heat and plastic deformation. The bit will be driven until a Z depth or load set for stage 1 is reached. This is usually when the bit meets the base layer of material. The bit will momentarily rub on this material per a set dwell time, generating heat before the bit continues to spin and descend into the material. Due to the similarity in the material of the bit and base material, the bit will plastically deform and heat up. When the bit reaches another Z depth or load set for stage 2, the FBJ machine will stop the driver with its brake, stopping the bit's rotation and descent. The heat and pressure between the bit and base material result in a solid-state bond. In the third phase, the driver retracts, leaving the consumable bit friction welded to the base material.

Bits generally consist of a "shank" and a "head" with a mating feature for interfacing with the driver. The head typically has a flange for pinching down the top layer. Some iterations of the bits have cutting features like a drill for removing the top layer of material. Some iterations have fewer or no cutting features and rely more on friction and force to push through the top layer. Bits were typically 9.53mm in diameter at the head, about 7.62mm in length, with a shank diameter around 7.11. Later versions were 11.25mm in diameter at the head, 3.89mm in length, with a shank diameter of 7.11mm.

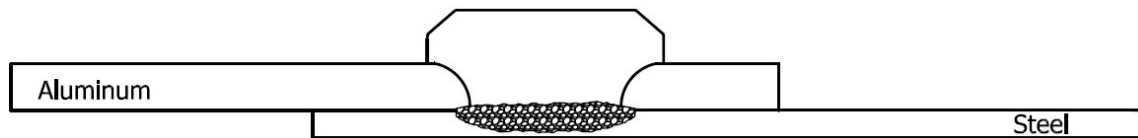


Figure 3-2: FBJ Diagram

Bit profiles were produced with an Okuma Space turn LB300-M CNC lathe. Mating features for interfacing with the driver were pressed into the head of the bits using a hydraulic press and dies.

3.4 Failure Modes in Tensile Testing

There are three relevant failure modes in the tensile tests that were performed for this research. First, there is an interfacial failure in which the shank of the bit shears at the weld bond site. In the case of a pure interfacial failure, the coupon materials are relatively unharmed.

Second, there is a material failure in which one of the coupons reaches the UTS of the material and tears before the weld fails. This would indicate that the weld is stronger than the coupon material.

Thirdly, there is a nugget pullout failure in which the base coupon material tears around the weld zone allowing the bit to pull the weld nugget through the hole in the top layer. This requires the most energy.



Figure 3-3: Failure Modes

3.5 Equipment and Testing

3.5.1 Equipment

To measure the peak load and fatigue life of FBJ joints in various scenarios, different orientations of FBJ joints were made. To measure peak load, the samples were pulled to failure with Instron or MTS equipment. To determine fatigue life, lap-shear samples were cyclically loaded at fractions of the weld strengths repeatedly until failure or a satisfactory number of cycles had been completed. An oven was used to cure adhesives. A corrosion chamber was used to test corrosion resistance.

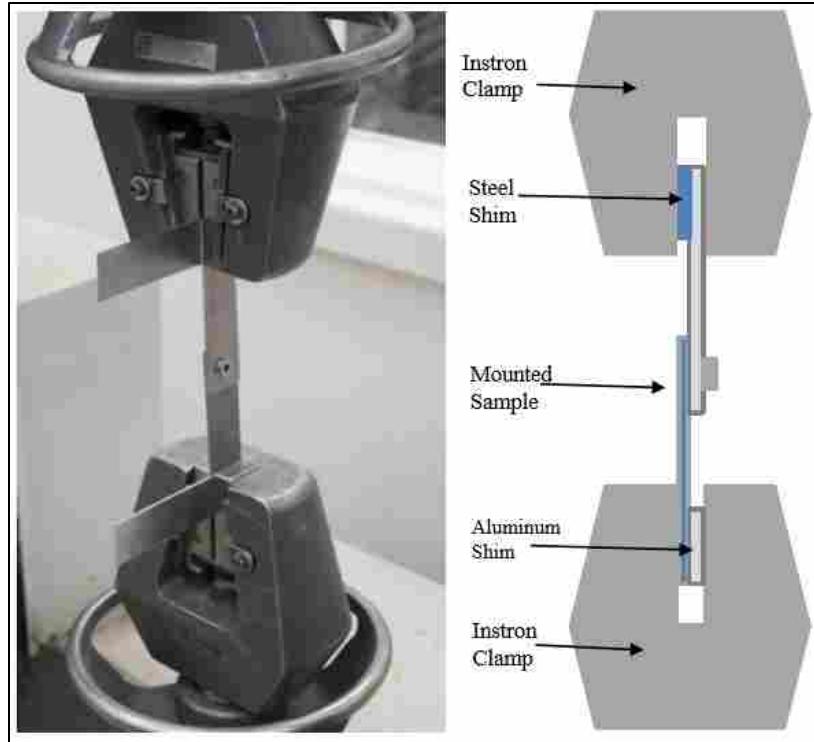


Figure 3-4: Method for Gripping Shear Specimens

3.5.2 Lap-Shear Tension

Lap-shear tension tests measure the strength of a FBJ joint in pure shear. Two 40 mm X 125 mm coupons are overlapped on the narrow ends by 20 mm, and a FBJ bond is made in the center of the overlap area.

In the case of corrosion samples using adhesives, to avoid an “edge effect,” the lower coupon is oversized to 50 mm instead of 40 mm and the top coupon is centered on the lower coupon while maintaining a 20 mm overlap. A layer of adhesive is placed between the coupons along with .254mm diameter glass beads before the FBJ bond is made. The sample is then cured in an oven for a prescribed time and temperature.

In the case of multi-weld samples, larger coupons are used. If there is no adhesive being used, then the coupons are widened to 120mm instead of 40 mm and two or more FBJ bonds are made along the centerline of the 20 mm overlap. In the case of a Multi-weld sample using adhesives, the width of the lower coupon is increased to 130 mm and the upper coupon is centered while maintaining the 20 mm overlap. The sample may receive multiple FBJ welds along the centerline of the overlap as well. The adhesive sample is then cured at the prescribed temperature and time.

These samples are pulled in an Instron or MTS to failure while using shims to keep the sample aligned in the pull direction.



Figure 3-5: Lap-Shear Tension Configuration

3.5.3 Cross-Tension

For cross-tension, larger coupons (150 mm by 50 mm) are used with predrilled 20 mm holes on each end for mounting in a fixture for destructive testing. The samples are bonded perpendicular to each other with their centers aligned. A FBJ joint is formed at the center of the

coupons. The sample is mounted in the Instron using custom fixtures which bolt through the holes in the coupons. The Instron pulls along the axis of the bit until failure.

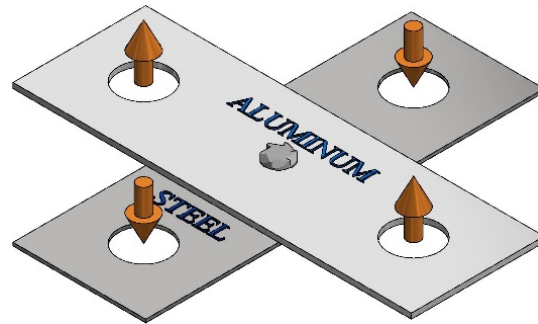


Figure 3-6: Cross-Tension Configuration

3.5.4 T-Peel

In T-peel two 40 mm x 125 mm coupons are bent 90 degrees so that there is a 35 mm straight section then a 5 mm internal bend radius and then an 80 mm straight section. The 35 mm section are joined together so that the 80 mm sections of each coupon are coplanar. The FBJ bond is made 20 mm from each of the three edges of the 35 mm sections. The sample is pulled until failure in an Instron grabbing midway up the 80 mm sections of each coupon.



Figure 3-7: T-Peel Configuration

3.5.5 Fatigue

For fatigue tests a lap-shear tension sample is created and put in a hydraulic Instron which repeatedly pulls the sample to a predetermined fraction of the average strength of the FBJ joint. This is repeated until a satisfactory number of cycles are completed or the sample fails.



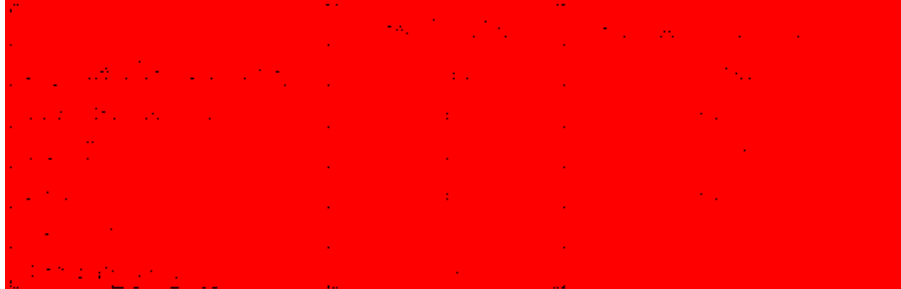
Figure 3-8: Hydraulic Instron for Fatigue Testing

3.5.6 Corrosion

For corrosion, lap-shear tension samples of interest, both large and small, with and without adhesive are placed in a controlled corrosive environment at Honda R&D. Periodically a sample of each type is removed and pulled until failure to determine how much strength has been lost to corrosion.

3.5.7 Automotive Standards for Spot Joint Performance

Table 3-1: Automotive Standards for Spot Joint Performance



4 RESEARCH RESULTS AND ANALYSIS

4.1 Process Improvement

Before completing the DOE, data on machine deflection were gathered using a dial indicator and using the spindle to apply pressure on the anvil of the machine. See Figure 4-1 for resultant deflections. These deflections make it difficult to predict actual Z depths. Bit geometries, such as the presence of cutting features, can greatly affect the weld pressure and therefore deflection and actual Z depth. Through trial and error, a new parameter can eventually be found to achieve the desired Z depth. The anvil or table was prone to rocking forward as well. This was addressed by placing spacers between the black H-frame and the anvil.

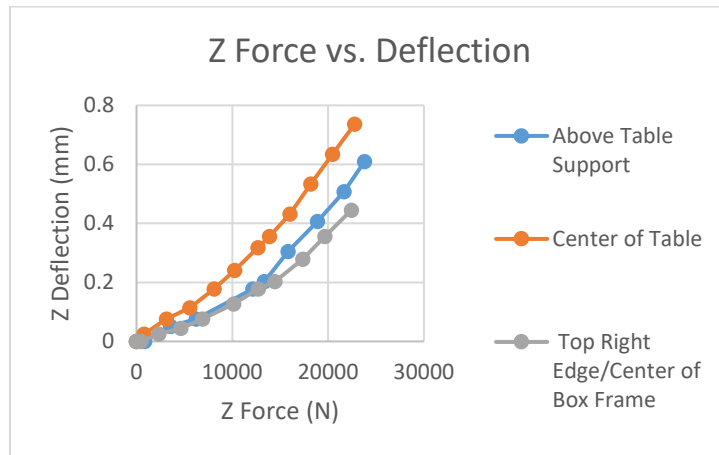


Figure 4-1: FBJ Machine Z Force vs. Deflection



Figure 4-2: FBJ Machine Points of Deflection Measurement

Previous FBJ research had used a simple pressure bar with a through hole for the bit and spindle to pass through and two bolts to apply pressure. These bolts were difficult to tighten evenly and caused it to clamp unevenly. The process for changing out coupons was also slow (at least a minute). To make a DOE repeatable and to make doing large numbers of samples feasible and also to progress the process towards a fully automated system, an automated clamping system was designed. Initially designs had mainly involved a structure mounting to the spindle bearing which supports a spring loaded or pneumatically actuated steel sleeve that would extend past the bit and apply downward pressure to the aluminum coupon as the spindle lowered in the Z direction. Because of the tight space in the box frame, the length of the spindle and the rotating nature of the spindle it was difficult to design a rigid, unobtrusive structure and to find springs or pneumatic cylinders strong enough and compact enough to deliver the needed clamping force while allowing for the spindle to travel in the Z direction. This method of clamping would also add more load to the anvil and increase deflection.

To counter these issues a design was proposed and built for a clamp that mounted to the anvil itself and actuated independently of the Z location of the spindle. A single 1,200 pound pneumatic double-action piston was sourced to provide the power to move two, parallel steel C frames along a rod through a guide bushing (not shown in the pictures). The parallel C frames allowed space for an automated bit feed system which was being developed by another research team member. Different clamp blocks could be bolted in as further driver design progress was made. Clamp location and pressure became more repeatable and the clamping and unclamping process was reduced to approximately 1 second which allowed for quick coupon changes for the DOE. Mounting the clamp to the anvil also isolated the clamp force so that it would create very little additional deflection in the anvil.



Figure 4-3: Pneumatic Clamp Before Installation on the FBJ Machine



Figure 4-4: Pneumatic Clamp Side View

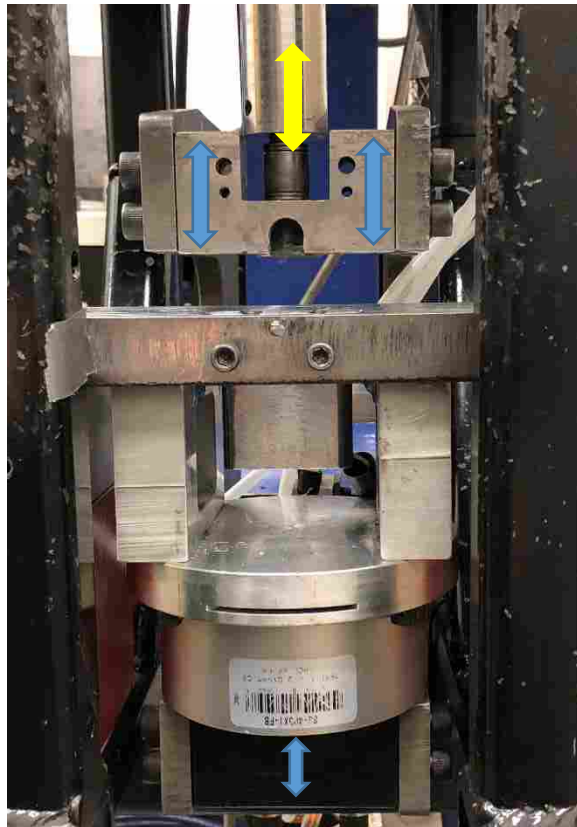


Figure 4-5: Pneumatic Clamp Actuated by Air Piston Underneath the Anvil

An additional source of variation was that the spindle itself would deflect laterally away from the machine. This caused the location and angle of the joints to vary. The deflection occurs because the spindle must be quite long to reach past T-Peel samples. To address this, first clamp blocks were designed with bushings to guide the driver to the target spot and resist that deflection. Though helpful, these bushings were not deemed a long-term solution because they wore out quickly. Next, drivers with rollers bearings were designed to slide axial into a hole in the clamp block as the spindle traveled in the Z direction. Bronze, oil embedded washers were used as thrust bearings to mitigate any friction from unaccounted for axial loads on the bearing. A view port was also included so that the joining process could be observed and recorded in real-time.

Another improvement was creating quick-change fixturing for coupons for the FBJ machine. Fixtures were created for lap-shear tension, cross tension and T-peel. This allowed for the order of the DOE samples to be easily randomized. Fixture changes were less than 30 seconds compared with the several minutes it used to take.

Bit production was also improved. Bits in previous research were machined and pressed. The press used a hardened D2 steel top die to create the drive features, but the lower die was unhardened which resulted in it deforming over time and allow variation in drive features. This was addressed by hardening the lower die as well. The 1018 steel bits required heat treatment to achieve sufficient hardness to create satisfactory welds. Previous research performed this task by creating stainless steel envelopes to seal out oxidizing atmosphere by making stainless steel pouches from foil on a roll. These pouches had poor seals and were difficult to quickly puncture for quenching in water. A half to a third of heat treatments failed because the quench was too

slow. Premade heat treatment pouches were purchased which created better seals and were much easier to puncture. Almost all heat treatments were successful with the premade pouches.

4.2 Design of Experiments

Before the Design of Experiments (DOE) could be performed, variability in weld strengths in both T-Peel and Lap-Shear needed to be addressed. T-Peel had an average peak load of 1800 N with STD 227 N. This allows for the lower end of the distribution to get dangerously close to the required 1500 N and occasionally dip below it. Lap-Shear had an average peak load of 8625 N with STD 1343 N. There is little danger of the load dropping below the required 5000 N, but the variability suggested the system had uncontrolled variables.

After Megastir performed maintenance on the welder, joints of comparable strengths could no longer be formed using the same parameters. To find valid parameters, weld depth was varied by .254mm increments until the depth resulting in the joint with the maximum peak load was found. An ideal depth was quickly found which was shallower than previous used by almost 1.27mm. The peak loads were consistently upwards of 11-12 kn upon further testing. Other improvements were made as well that will be discussed later. The failure mode changed from material failure in the aluminum to nugget pullout. In some cases, the nugget pullout tore the steel all the way to the end of the steel coupon. The average peak load improved to 12203 N with STD 310 N.

Table 4-1 : Lap-Shear Peak Loads with New Parameters

Sample #	Peak Load (N)
2016-09-22-06	12361
2016-09-22-07	12490
2016-09-22-08	12197
2016-09-22-09	12090
2016-09-22-10	12490
2016-09-22-12	11591
AVG	12203
STD	310

T-Peel peak loads also improved to consistently being over 2 kn. Almost all failures were nugget pull outs. As can be seen in Table 4-1, the average peak load improved to 2170 N with STD 70 N which is in no danger of dipping below 1500 N.

Table 4-2: T-Peel Peak Load with New Parameters

T-Peel Peak Load With New Parameters	
Sample #	Peak Load (N)
2016-09-13-01	2241
2016-09-13-02	2228
2016-09-13-03	2208
2016-09-13-04	2071
2016-09-22-11	2101
AVG	2170
STD	70

To consider FBJ for bonding 1.2 mm thick GADP1180 and 2 mm thick AA7085 in a mass production setting for the automotive industry, effective weld parameters needed to be established for this material combination so that joints will meet requirements for lap-shear, T-peel and cross-tension. Up until this point it was assumed that achieving ideal parameters for one of these tests would optimize the results for the other tests. This assumption was questioned to ensure that T-peel requirements can be consistently achieved while still achieving other requirements. It was suspected that each configuration (T-peel, lap-shear tension, and cross tension) would benefit the most from different parameters. It was also hoped that general relationships between parameters and peak load can be determined for each test.

To determine the relationship between weld parameters and the peak loads for lap-shear, T-peel and cross-tension, a DOE was performed using 1.2 mm thick GADP1180 and 2 mm thick AA7085-T76 coupons and varying the weld Z plunge rate and plunge depth on the second stage which is the stage where the actual weld is formed. A full factorial DOE was performed using three levels for each of the variables. Five replications were performed per parameter combination for lap-shear and cross-tension tests. Ten replications per parameter combination for T-peel were performed because previous tests had highly variable results. Previous research revealed that a faster RPM results in higher peak loads. As such, the RPM for all tests was left at 4000 for both stages of the weld cycle which was the maximum RPM the experimental FBJ machine was capable of.

Table 4-3: DOE Variables

Level	Z Depth in mm (inches)	Z Feed Rate in mm/Min. (In/Min)
High	-5.21 (-.205)	152.4 (6)
Medium	-4.95 (-.195)	114.3 (4.5)
Low	-4.69 (-.185)	76.2 (3)

Parameter combinations and weld configuration (i.e. lap-shear, T-peel, cross-tension) order was randomized using a random number generator.

FBJ bits were produced out of 1018 steel in a three-step operation using a CNC lathe to machine the cutting features and general shape of the bit followed by a cold heading operation to press drive features into the head and then finally a heat treatment procedure to increase the bits hardness to 40-45 HRC. Bits were hardened in batches and batch lot numbers were tracked. Bits were used from the first batch first and then the second and so on.

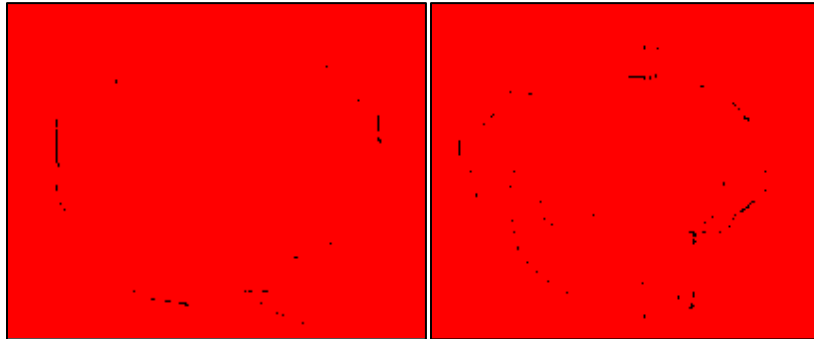


Figure 4-6: DOE FBJ Bit Design

Welds were performed using the randomized schedule one after the other until all welds were complete. Samples were pulled by weld configuration type by an operator using an Instron tensile tester without knowledge of the parameter types to avoid bias. Samples were pulled at a

rate of 10.16mm/minute. Standard grippers were used to pull the T-peel and lap-shear samples. A custom fixture was used to pull the cross-tension samples.

Peak loads and failure modes were recorded for each sample. Weld thickness, the distance from the bottom of the steel coupon to the top of the head of the bit, was measured with calipers before destructive testing of each sample. Max weld Z force was also recorded from a load cell in the anvil of the FBJ machine during the welding process. Due to a limited sampling rate of 17 Hz, a short cycle time of approximately 2 seconds and a sharp pressure spike, recorded max weld forces were likely not accurate.

Statistical analysis was performed to determine the relationship between the varied weld parameters and peak load in each configuration. Analysis was also performed to determine the relationship between the parameters and the failure modes with the hope of finding parameters that would favor nugget pullout failures which absorb more energy in an impact. Weld thickness was compared to programmed weld depth to account for possible deflection in FBJ machine's frame during the weld cycles since the machine runs off Z height offsets instead of pressure feedback. Max weld Z force was compared to peak loads as well with the hope that appropriate forces could be determined for future machine designs that could use force control instead of Z displacement.

The raw data set is too large to represent effectively in this paper. The statistical analysis and main conclusions can be shown with three graphs showing peak load graphed in kN with Z weld plunge depth in inches on the X axis and Z plunge feed rate in inches per minute on the Y axis. Outliers were removed from the data sets to create these charts.

In Figure 4-7, lap shear samples made with a shallow Z depth and a high feedrate achieved the highest peak loads. When the weld forms, a ring of steel flash is generated around the weld and underneath the aluminum which heats up and displaces aluminum which would otherwise be pinched under the bit of the friction bit and contribute to the strength of the joint. Since plunging the bit farther into the weld will generate more heat and displace more steel which will then increase the size of the steel flash and displace more aluminum, deeper Z depths will result in less aluminum to resist loads along the axis of the bit resulting in lower peak loads. Although in lap shear, the welds experience a peeling force because the aluminum and steel bend under the shear load. This makes the thickness of the aluminum underneath the head important even in lap-shear.

Faster feedrates result in greater weld pressure and faster heat generation for the weld which means less heat is required for the weld since less heat will dissipate into the surrounding steel and aluminum before the bond is made. Excess heat effects the grain structure around weld by increasing the size and severity of the Heat Affected Zone. Excess heat also results in more unwanted changes in the grain structure of the bit, parent material and weld itself.

Reducing temperature, shearing forces and crack initiation points in the aluminum appear to maintaining joint strengths. In general, bit-to-steel welds are strongest when the weld reaches full depth quickly to reduce thermal influences on the surrounding metals. This requires a machine capable of the additional spindle torque and Z force. Hopefully future machines will have the Z load feedback capabilities to begin control the welds by Z force instead of Z depth. This may help overcome variation issues in setup, bit dimensions and coupon thicknesses.

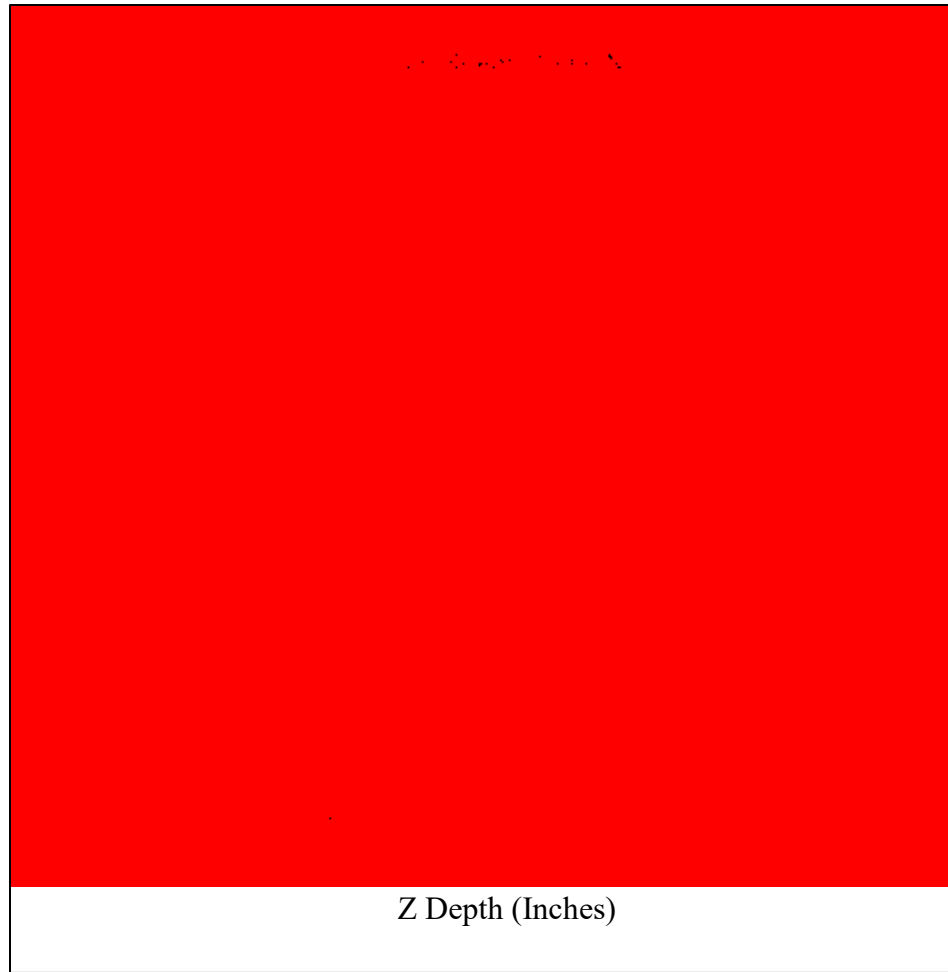


Figure 4-7: Lap-Shear Tension IPM to Z Depth Relationship in kN

In Figure 4-8, cross tension samples made with a deep Z depth and a high feedrate achieved the highest peak loads. The deep Z depth contradicts the reasoning that explains the results for lap shear. It is important to note this relationship, but the cause is currently unknown. A deeper Z depth should result in the generation of more steel flash underneath the aluminum which would undercut critical aluminum underneath the head of the FBJ bit. The theory had been that thinning out the aluminum in this manner would negatively affect the ability for the aluminum to resist the shear forces along the axial direction of the bit. The empirical result calls this theory into question.

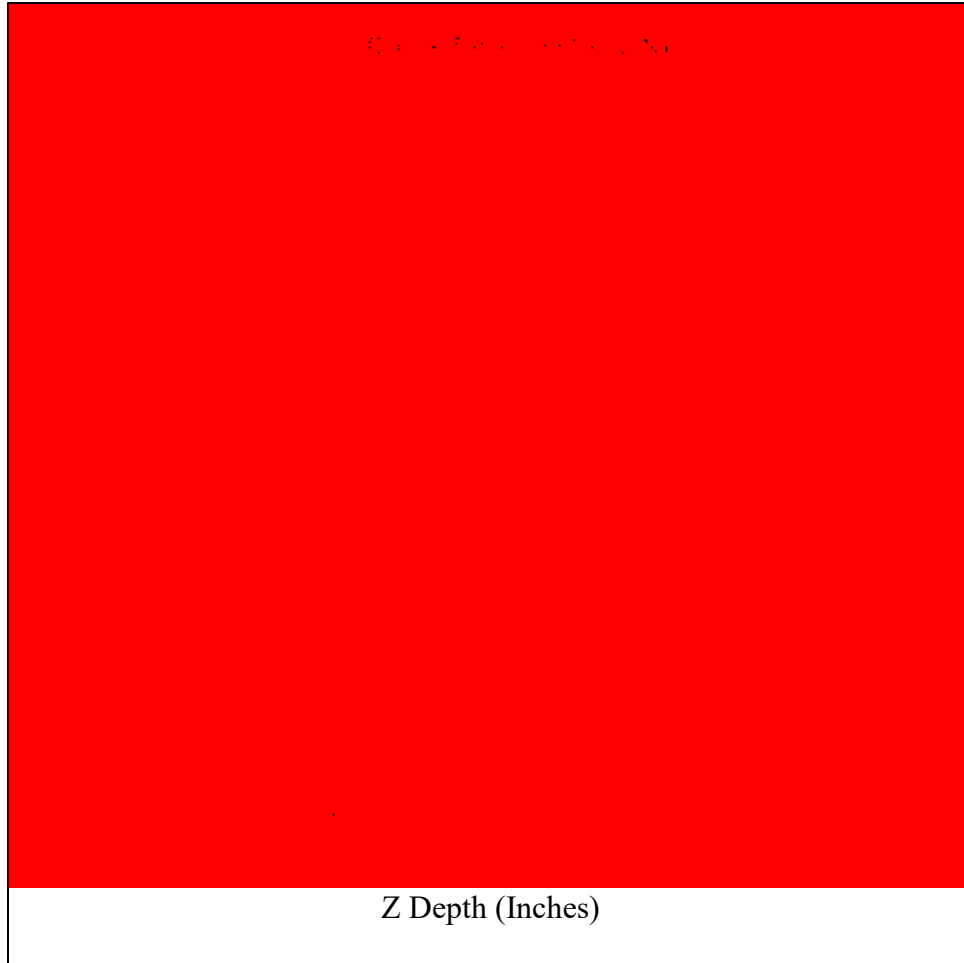


Figure 4-8: Cross Tension IPM to Z Depth Relationship

In Figure 4-9, T-peel sample peak loads had little correlation with Z depth. In fact, local maximums were found on the extremes of high and low Z depths compared to medium. High feedrate continued to prove to be beneficial to peak loads for the same reason that a faster feedrate generates more heat for the bond faster so heat does not have time to dissipate as much away from the bond region before the bond is formed. The limited testing suggests that T-peel peak load repeatability increases with higher feedrate and shallower Z depth.

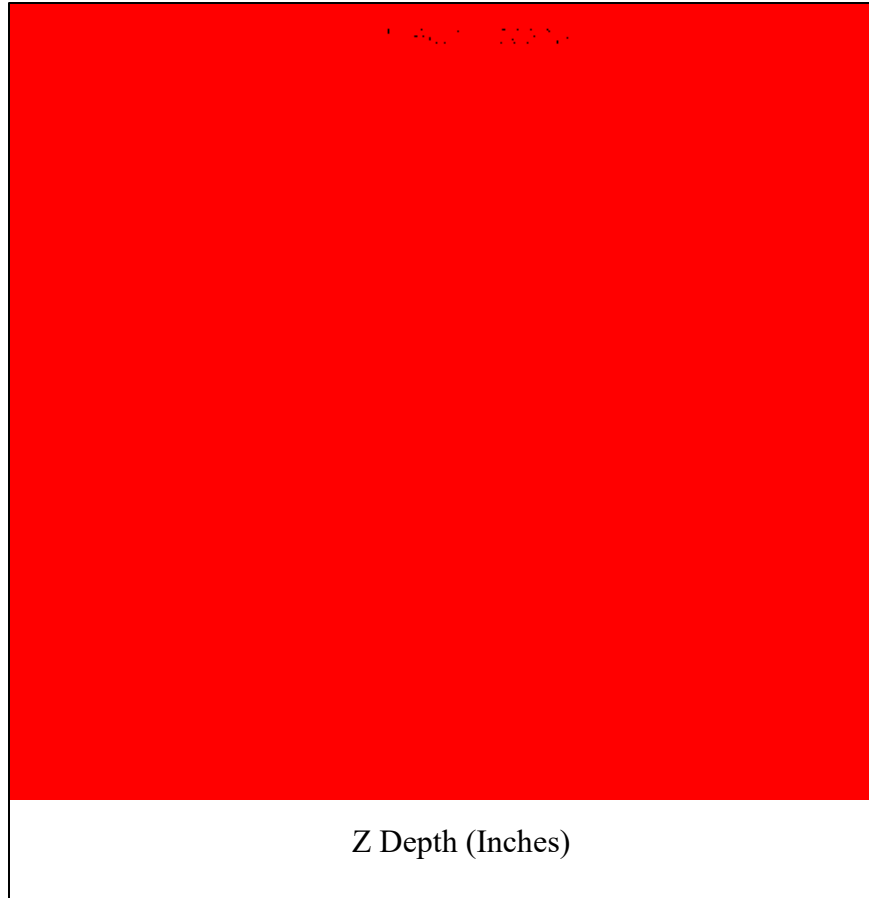


Figure 4-9: T-Peel IPM to Z Depth Relationship

A weld parameter was found that passed all the requirements in every test in all configurations. This weld parameter, which happens to be the parameter that has been used for the past year, passed all tests without any outliers. The average results for this parameter, which used a shallow depth and medium federate, are shown in the Table 4-4 below. This parameter set might still not be the optimal choice. If outliers can be addressed, settings with high feedrates would generally have higher peak loads. Something in the current equipment, bit design or process parameters is leading to low outliers. This still remains an area of interest and research.

Table 4-4: Average Peak Loads for Parameter Meeting All Requirements

Configuration	Peak Load Average (N)	Requirement (N)
T- Peel	1897	>1500
Cross Tension	4831	>1500
Lap-shear	10714	>5000

4.3 Fatigue

The results for fatigue testing are tabulated in Tables 4-5, 4-6, and 4-7. Welds were made with the same style of bit as was used in the previously mentioned DOE. Lap-shear tension samples were cycled between a range of tensile loads at 27 Hz with an R value of 0.1. Failure mode for specimens cycled between 0.5-5 kN can be seen in Table 4-5. All samples had both weld nugget and aluminum material failures. They survived an average of 24,251 cycles with a standard deviation of 1,238. The failure mode of 0.25-2.5 kN was all cracking of the aluminum. It is suspected that the aluminum failed first because the steel was not taken beyond its fatigue limit. These samples survived an average of 90,235 cycles with a standard deviation of 5,841. The samples cycled at 0.25-2.5 kN survived an average of 751,774 cycles with a standard deviation of 99,575. At higher loads, the steel is more prone to failing around the weld nugget presumably because the fatigue limit is being surpassed. At lower load testing, the failures were almost exclusively in the aluminum which is likely because aluminum does not have a fatigue limit and will therefore weaken with every cycle.

Table 4-5: High Load Fatigue Results

Fatigue: 0.5-5 kN, 27Hz R=.1		
Sample #	Cycles	Failure Modes
2016-08-30-01	22503	Nugget, Al
2016-08-30-02	25218	Nugget, Al
2016-08-30-03	25032	Nugget, Al
Average	24251	
std.	1238	

Table 4-6: Medium Load Fatigue Results

Fatigue: 0.125-1.25 kN, 27 Hz R=.1		
Sample #	Cycles	Failure Mode
2016-09-22-02	890882	St
2016-09-22-03	609949	Al
2016-09-22-04	762912	Al
2016-09-22-05	743353	Al
Average	751774	
std.	99575	

Table 4-7: Low Load Fatigue Results

Fatigue: 0.25-2.5 kN, 27 Hz R=.1		
Sample #	Cycles	Failure Mode
2016-08-30-04	97814	Al
2016-08-30-05	89290	Al
2016-08-30-06	83600	Al
Average	90235	
std.	5841	

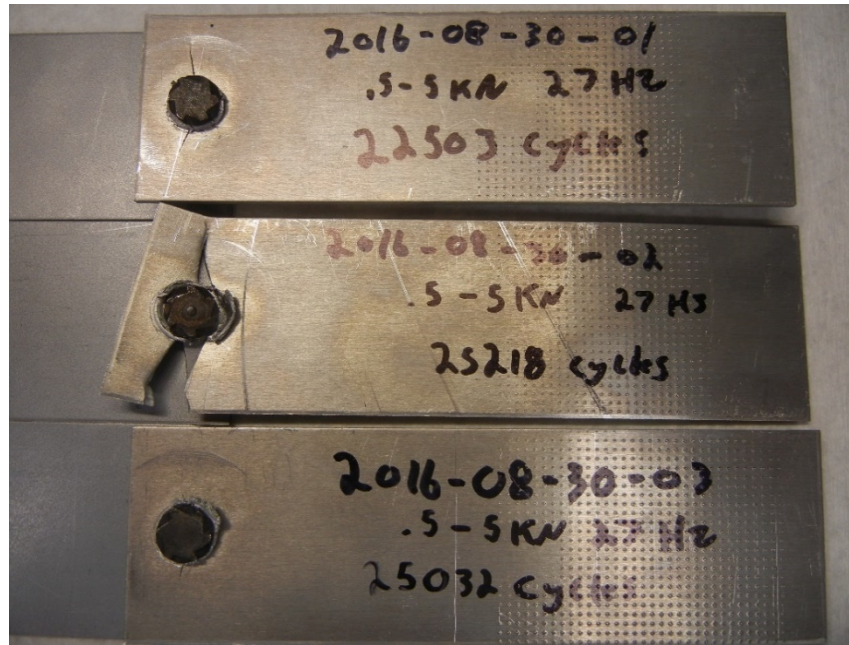


Figure 4-10: .5-5kN Fatigue Sample Nugget Pullout and AA Material Failure

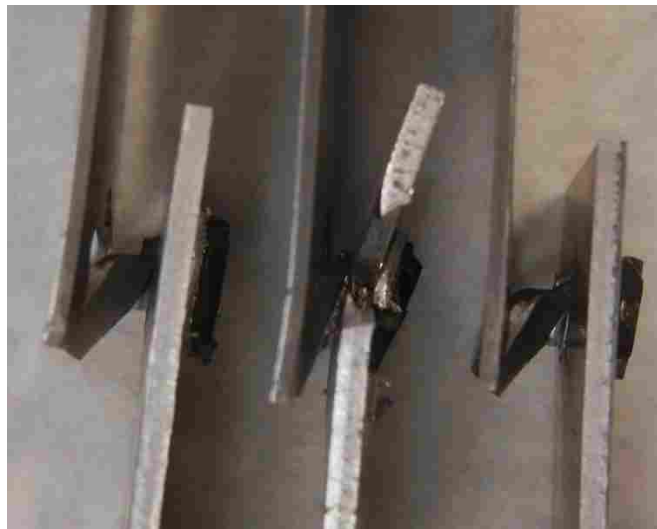


Figure 4-11: .5-5kN Fatigue Samples with Nugget Pullout Failure



Figure 4-12: .5-5kN Fatigue Sample Weld Nugget Pullout Failure

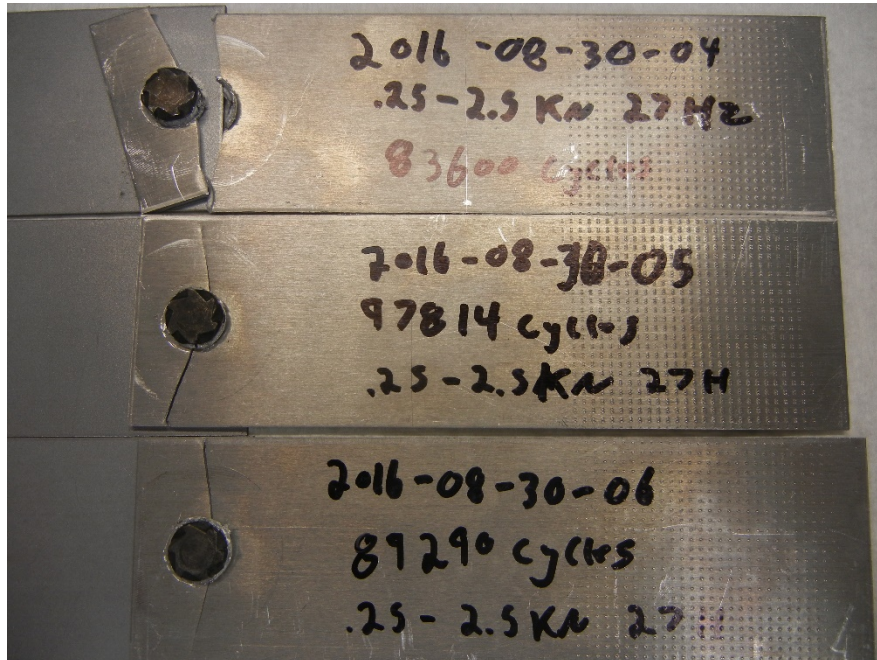


Figure 4-13: .25-2.5kN AA Material Failure Only in All Three Samples

4.4 Multi-Weld Lap-Shear Tensile Test Samples

Sponsors expressed concern that consecutive joints made on the same piece may apply unwanted loads on other joints in the same piece and reduce the strength of the joints. To test this scenario, five lap-shear samples were initially made with the following features to see if multiple welds in the same sample will result in additive peak loads:

- 120 mm X 125 mm coupon size
- Joined along the 120 mm edge
- 20 mm overlap
- 3 FBJ welds spaced 40 mm apart (center to center), 10mm from the joined edge, 20 mm from the long edge
- Welds were done sequentially across the coupon

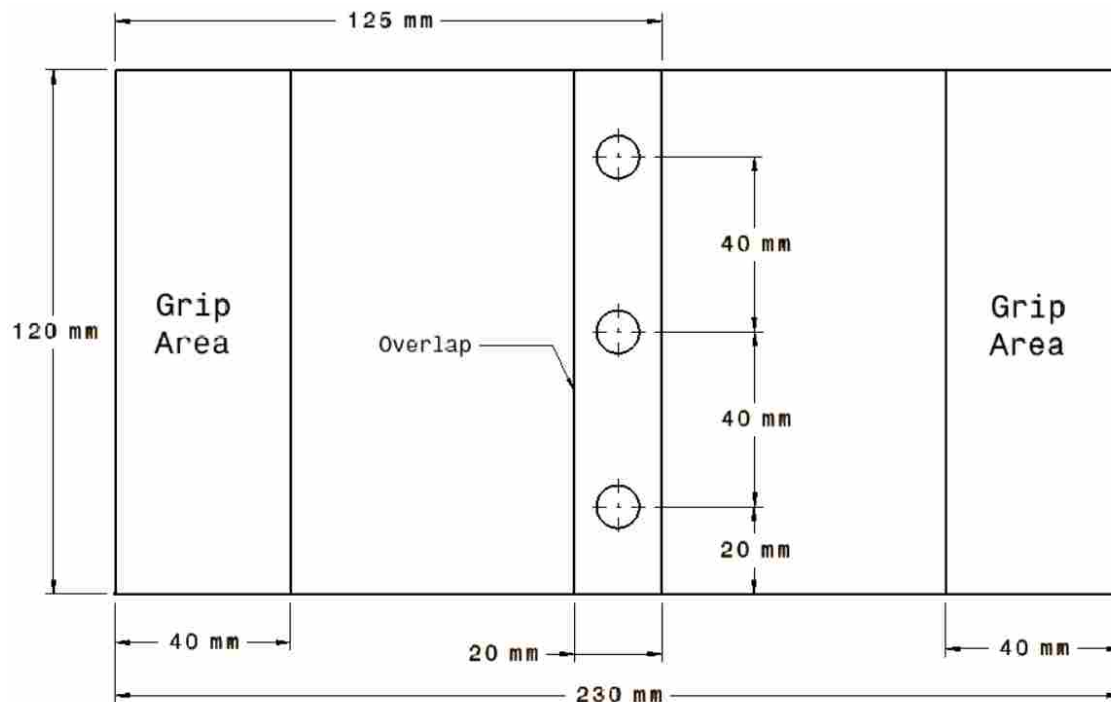


Figure 4-14: 3 Weld, 40mm Spacing on 120mm Wide Lap-Shear Specimens

An MTS with 100 mm wide hydraulic grippers was used to pull the samples to failure. The outermost 40mm of the aluminum and steel coupons were gripped for pulling. The results are tabulated in Table 4-8.

Table 4-8 Multi-Weld Lap-Shear Tensile Test Results

Large Coupon Sample #	Peak Load (N)	Individual Weld #	Failure Mode
L-2016-10-20-00	30838	2016-10-20-02	Al
		2016-10-20-07	Al
		2016-10-20-12	Al
L-2016-10-20-01	32482	2016-10-20-03	Al
		2016-10-20-08	Al
		2016-10-20-13	Al
L-2016-10-20-02	30127	2016-10-20-04	Al
		2016-10-20-09	Al
		2016-10-20-14	Al
L-2016-10-20-03	24173	2016-10-20-05	Al
		2016-10-20-10	Al
		2016-10-20-15	Interfacial
L-2016-10-20-04	25624	2016-10-20-06	Al
		2016-10-20-11	Interfacial
		2016-10-20-16	Nugget Pullout
Average	28649		
Average of "good" welds	31149		
Average of "bad" welds	24899		

Two of the samples appear to have had at least one bad weld in them. The welds with interfacial failure modes appear to have been shallow, weak welds based on steel discoloration,

failure mode, and premature failure. In the case of the one nugget pullout, it appeared to be the last weld to fail. When the weak welds failed, the good welds were forced to carry additional load and failed soon after.

Multiple FBJ welds appear to be mostly additive in peak load capacity in lap shear. When the weakest weld fails, the load it was carrying is distributed to the other welds which usually exceeds the peak loads of those welds. It is difficult to tell for certain if the welds that failed prematurely failed because they were simply “bad” welds or if they became bad welds because of the multi-weld scenario. The failure mode in multi-weld samples is usually aluminum material failure which is different from the single weld samples. The single weld samples bend and turn into a slight peel situation instead of pure shear. This peeling initiated tears around the weld nuggets. With more material and more welds, the multi-weld samples are stiffer and do not allow the coupons to bend and create the peel situation and so tearing around the nuggets is not initiated before the aluminum fails. In the case of the one nugget pullout failure mode, a weak weld in the middle had failed and the aluminum on the other weld began to fail so the sample was able to bend and put the remaining weld in a peel situation which initiated a tear and the subsequent nugget pullout.

Figure 4-15 shows one of the samples with all “good” welds and demonstrates the additive peak loads and uniform failure mode. Figure 4-16 shows one of the samples with a “bad” weld. The “bad” weld may have held almost no load, so considering the two remaining “good” welds, the result still suggests additive peak loads. Again, it cannot be determined for certain if the weak weld was simply an outlier or if it was caused by the multi-weld scenario. Figure 4-17 shows a sample in which all three failure modes are present because a “bad” weld in the center gave way first. The aluminum on the right weld gave way second and the last weld

held well, but without the other welds to provide more stiffness the coupons bent and lead to a peel scenario which lead to a nugget pullout. This suggests that the failure mode of FBJ joints is affected by the presence of and failure of nearby welds.

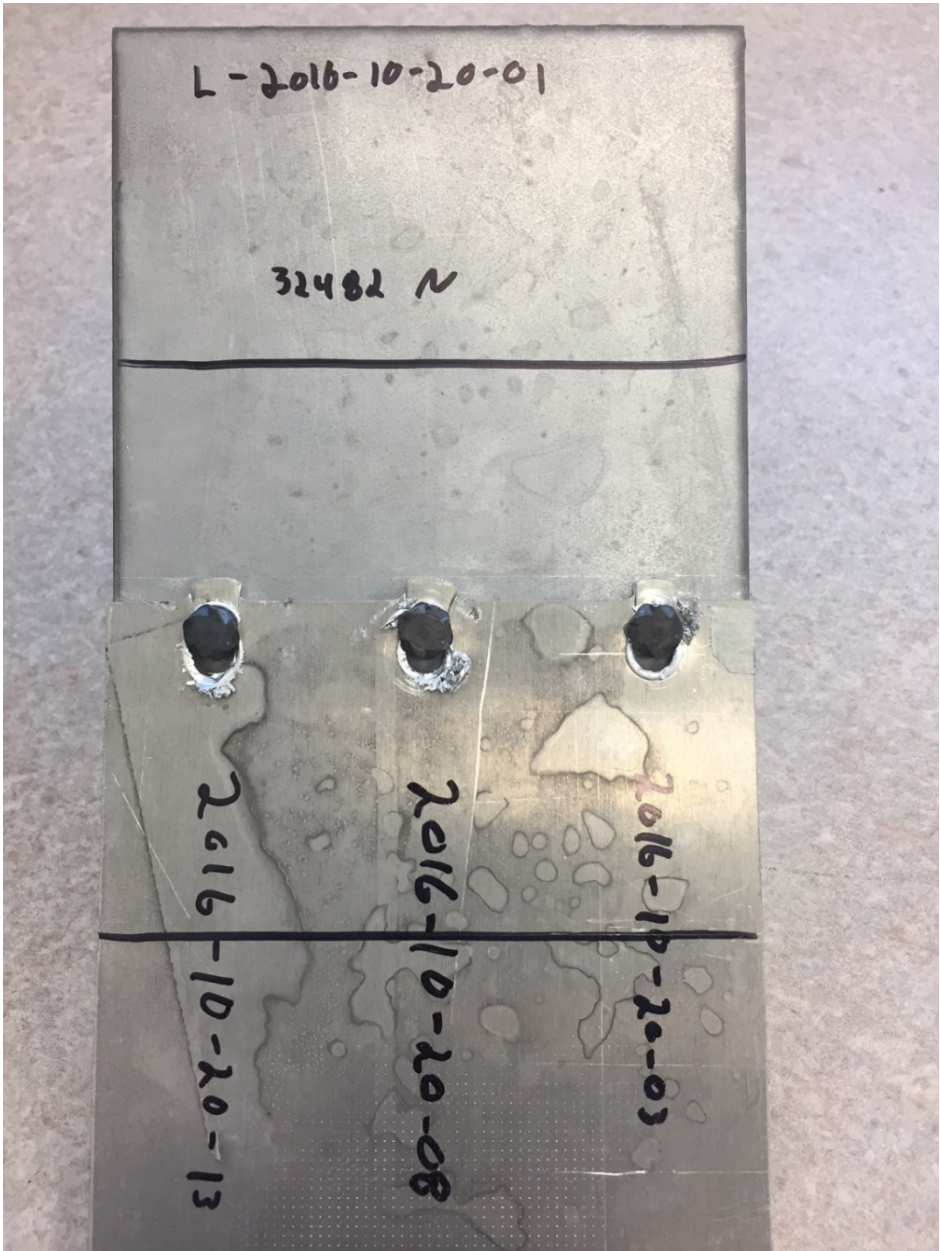


Figure 4-15: Example of "Good" Welds with Aluminum Only Failure Modes

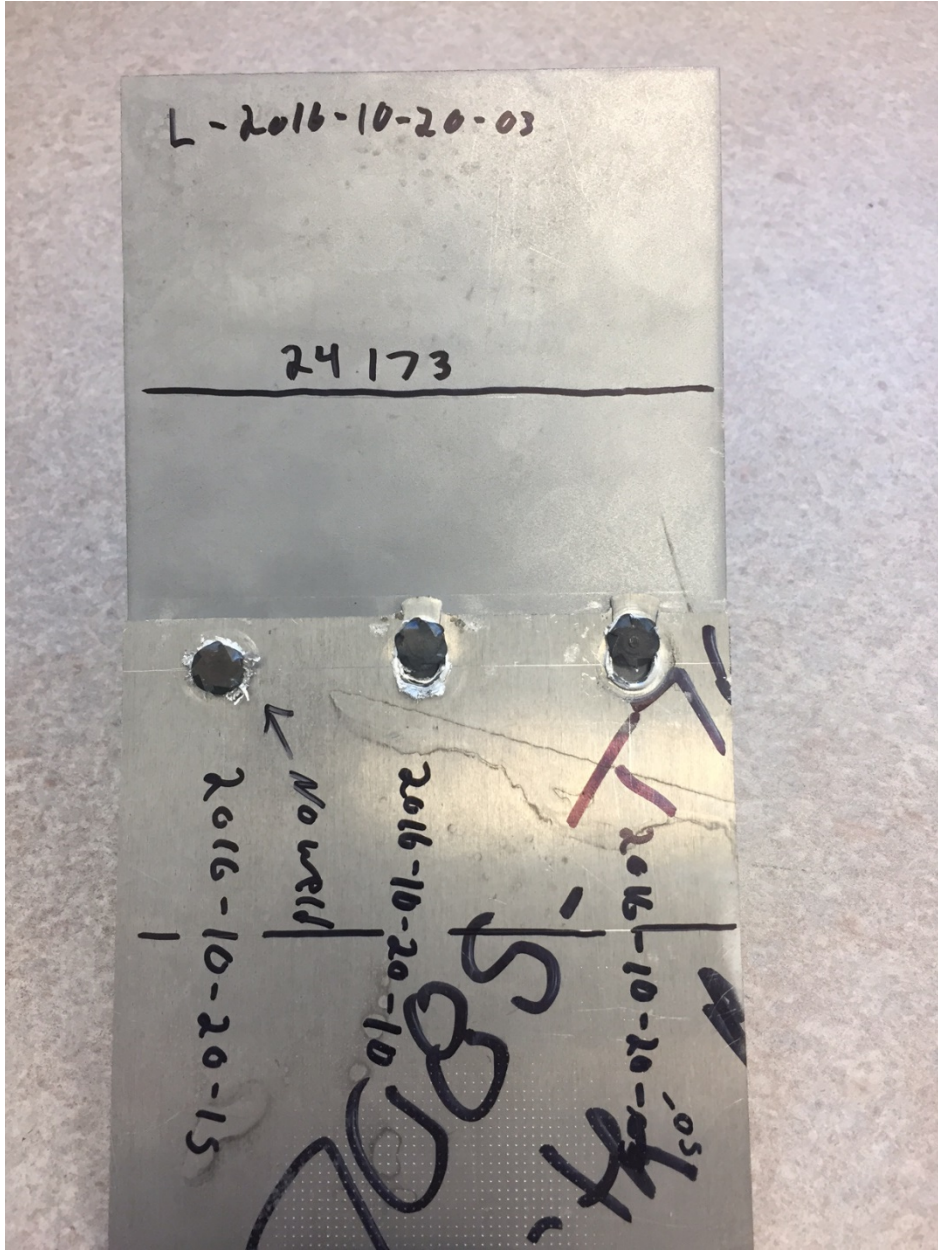


Figure 4-16 "Bad" Weld with One Interfacial Failure and Two AA Failures

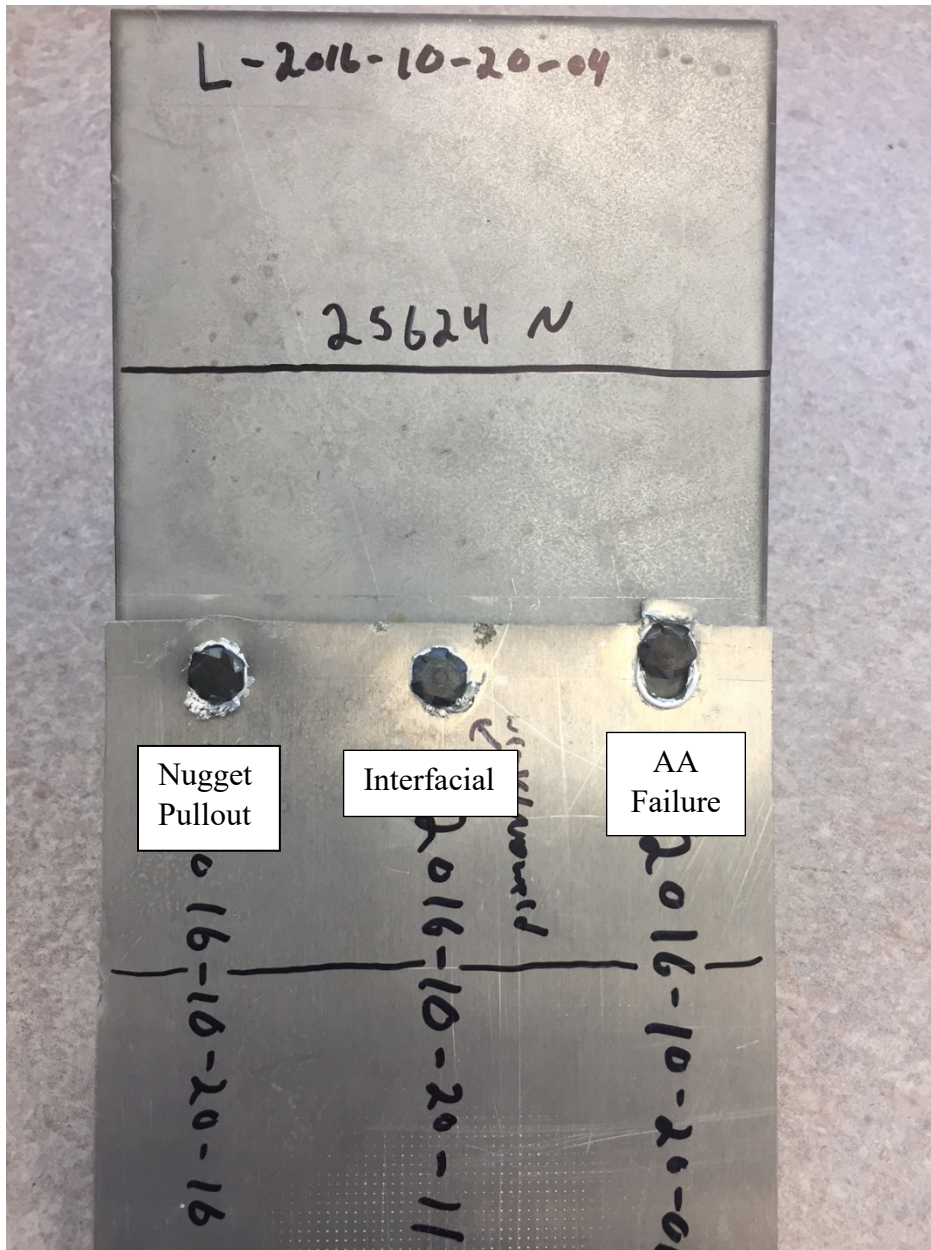


Figure 4-17 "Bad" Weld Failure Modes

Additional testing was done using two joints per specimen but varying the spacing between the welds from center to center at 60mm, 70mm and 80mm. Initially these tests were performed on coupons only 100mm wide because there were concerns that since the hydraulic grippers were only 100mm wide there would be confounding distortions of load conditions.

There were no observed problems with this change for the 60 and 70mm spacings, but for the 80mm spacings this put the joints within 10mm of the edge of the coupon which was too close to edge of the specimen. The aluminum failed prematurely, tearing out towards the sides of the coupon instead of failing along the bonded edge. The 80mm spacing specimens were repeated on coupons that were 120mm wide. This increased the distance of the joints from 10mm to 20mm and the problem did not occur again. The distance from the joint to any edges of the coupons is important. Peak loads in consecutive joints on the same work piece continued to be mostly additive as can be seen in Table 4-9.

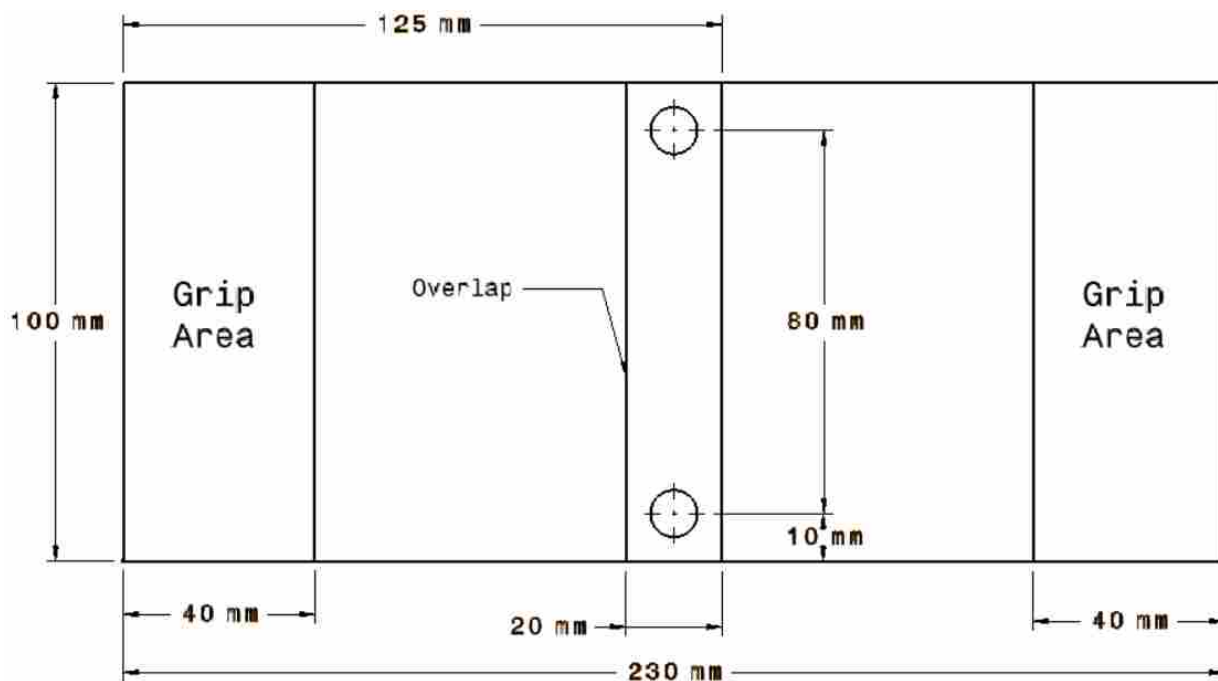


Figure 4-18: 2 Weld, 80mm Spacing on 100mm Wide Lap-Shear Specimens

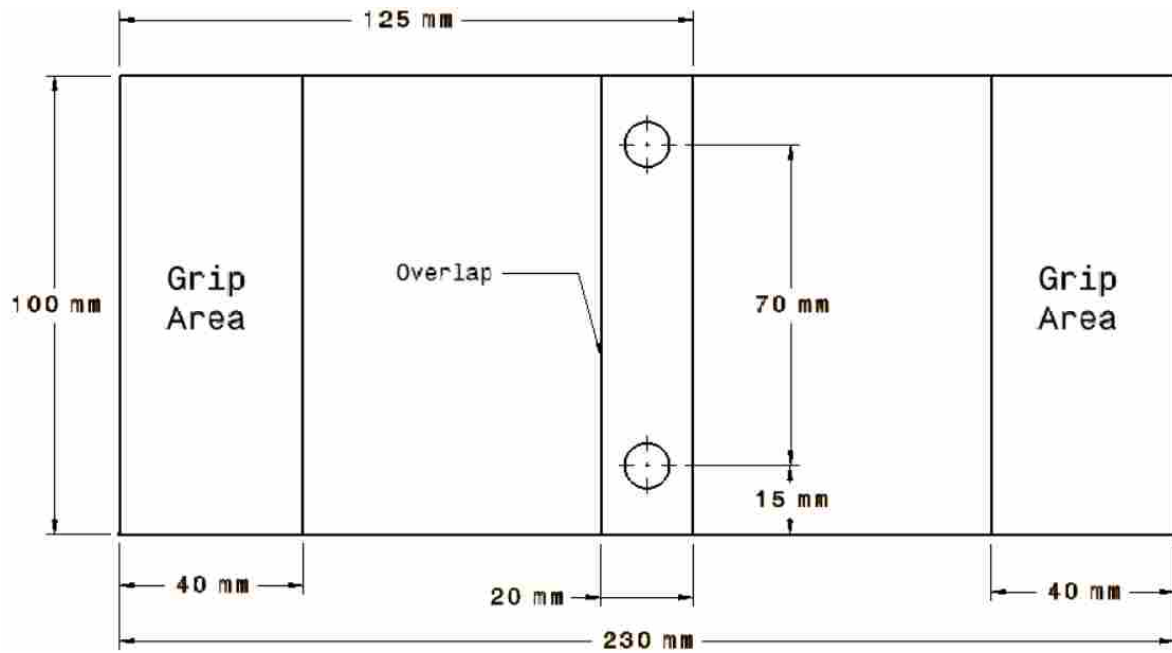


Figure 4-19: 2 Weld, 70mm Spacing on 100mm Wide Lap-Shear Specimens

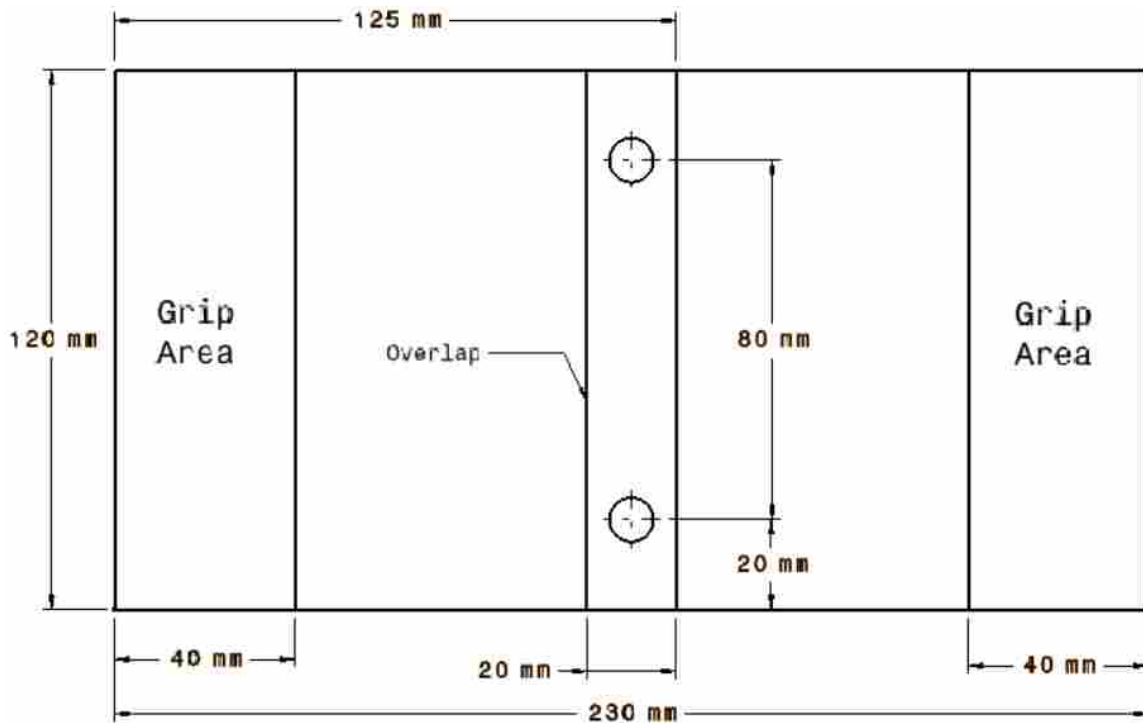


Figure 4-20: 2 Weld, 80mm Spacing on 120mm Wide Lap-Shear Specimens

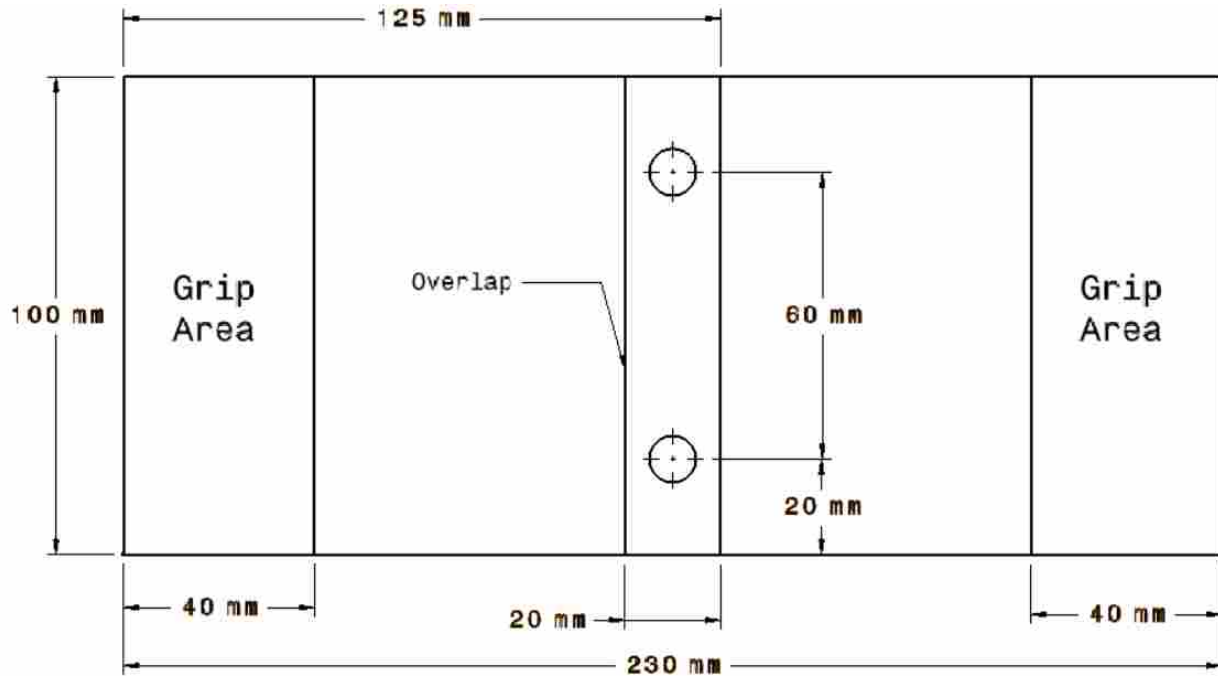


Figure 4-21: 2 Weld, 60mm Spacing on 100mm Wide Lap-Shear Specimens

Table 4-9: Multi-Weld Lap-Shear Peak Loads at Different Spacings

Spacing of 2 welds (mm) on width of coupon (mm)	Average Peak Load (N)	Sample STD (N)	Average Per Weld (N)
80 on 100	17988	546	8994
80 on 120	22542	318	11271
70 on 100	21319	831	10660
60 on 100	21435	673	10717

There were concerns about the load paths through the large coupons with multiple joints. A test using Digital Image Correlation (DIC) was used to investigate the stresses in a multi-weld sample. High resolution pictures were taken rapidly of the sample while it was being pulled to failure. A spray-painted speckle pattern provided reference points that stretched as the sample was strained. Special software analyzed the distortion of the speckles to estimate the strain. The sample was prepared in the same manner as the other multi-weld samples. As can be seen in

Figure 4-22, the stresses were concentrated on the edge side of the bit up till failure.

Unfortunately, tracking of the steel was not possible during this test because once the aluminum stretched the software could no longer track the distortion on the unpainted area. Performing DIC on the backside of the steel would have shown the stress in the steel. However, based on the results seen in the aluminum it is likely that similar stress would be seen on the steel, but to a lesser extent because of its higher strength. The center weld was an interfacial failure so once it failed there was no change in the DIC results in that area. The other welds were aluminum material failures. The DIC results suggest that the load path through the large coupons is simple and predictable with most of the strain occurring on the edge side of the FBJ joint. Figure 4-22 is the last DIC image with observable change.

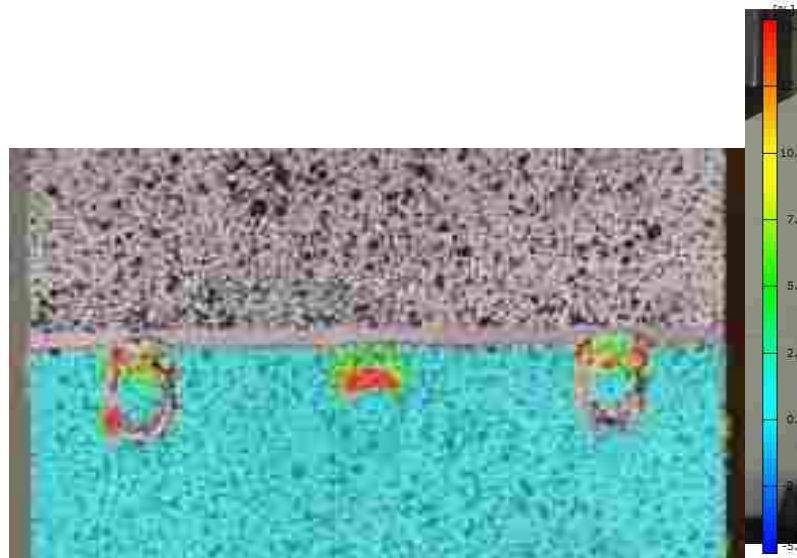


Figure 4-22: DIC Results for a Multi-Weld Sample with 3 FBJ Joints

4.5 Bit and Driver Design

To improve the surface finish and hopefully eliminate the aluminum flash which was generated around the head of the FBJ head, several bit designs were tested with the theory that features on the bit could be used to remove flash. The previous bit designs had very little relief angle behind the cutting edges of the tips of the bits so the leading faces of the bits were doing more rubbing than cutting. Because of the crude nature of the pressing operation to form the driver features into the heads of the bits, the cutting edges on the sides of the flutes are often deformed and dulled. The bits were also positively tapered which means that with dull flutes, the bit was pushing more aluminum out of the way as the bit went deeper instead of cutting the aluminum. It was believed that this action was responsible for the ring of aluminum flash that usually forms around the bit head. It was hoped that cutting features could be improved by either creating a better die for pressing the bits which would protect the flutes, incorporating more of a relief angle behind the cutting lips, or adding a third flute. None of these efforts had any appreciable impact on flash. More bit designs were tried.

Bits were tested with negative tapers along the shank of the bit with the hope that flash would be pushed down by the head of the bit to fill in the gap left behind instead of displacing as much aluminum. Another variant had a small step on the underside of the head with the hope that it would shear off flash that was only attached near the shank. Initial tests used a CNC mill to drill with a 1018 rod with the desired bit geometries machined into the end of it. As can be seen in Figure 4-23, a wide, shallow step underneath the head of the bit contacted the aluminum and sheared off most of the aluminum flash which can be seen flying away from the spindle. These preliminary tests partially validated the concept. Subsequent tests with actual bits could not replicate the results.



Figure 4-23: Testing FBJ Cutting Features with CNC Mill

Another bit design attempted to cover the flash instead of removing it. Because the bits still had cutting features which created stringy flash and debris, it did not seem feasible to cover the flash if cutting features were to be kept. Figure 4-24 shows how the flash still stuck out from under the cap. The cap captured chips that would have otherwise been free from the joint. The cap also made the bit unacceptably large.

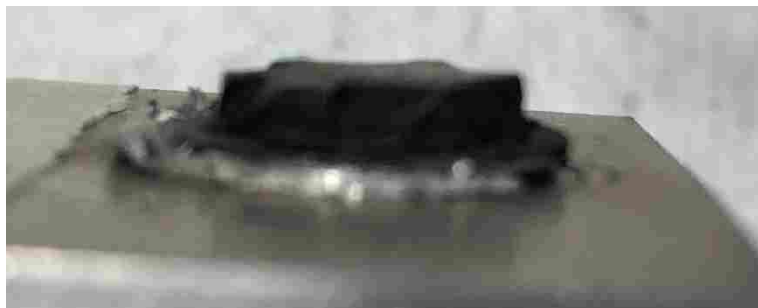


Figure 4-24: FBJ with Cap to Cover Aluminum Flash Instead of Removing It

The next bit designs were focused on improving the cutting features so that only clean chips which could be easily evacuated would be produced. The cutting flutes were extended along the full length of the shank of the bit. Special efforts were made to ensure the dies did not damage the cutting features during pressing. However, none of these ideas resulted in a noticeable improvement in flash generation.

After seeing no improvements in flash from the cutting feature improvements, a bit was made with no cutting features at all. The bit still had the nub on the tip of it to prevent the bit from “walking” on contact with the aluminum and to help scrape away the galvanized coating on the steel. As can be seen in the tabulated results in Table 4-10, cutting features appear to have no benefit in terms of maximum achievable peak loads. The first weld had the greatest peak load to date though only by a few hundred Newtons. As can also be seen, there is still considerable variation, perhaps more.

Table 4-10: Lap-shear Peak Loads of Bits with No Cutting Features

Sample #	Peak Load (N)	Failure Mode
2016-12-15-00	12784	interfacial
2016-12-15-01	12570	big nugget pull out
2016-12-15-02	9808	interfacial

Before the most recent bit design was developed, a few clamp designs were tested which are explained in section 4.6.

Attempts to put all flash removal features in the bit geometry were abandoned and instead a new idea was tested. A dedicated cutter system seemed like the only solution which will be addressed in detail in section 4.6. A separate cutting system provided the opportunity to try a different bit design, one in which the bit would be shorter and driven completely flush with the aluminum, since flash would be cut and removed anyways. This would make FBJ surface finishes comparable with self-piercing rivets.

The external drive features of the previous bit designs were not conducive to driving a bit flush since the external drive features are deep and would necessitate pushing the driver into the aluminum. An internal driver was needed. The concept was tested using the heads of countersunk Torx Plus machine screws. They were found to have similar enough properties to some of the materials used for previous bits. Previous FBJ research used Torx Plus drivers so components were already on hand to quickly prototype a driver. A simple steel wiper was machined into the driver to provide a crude cutting system.

Initial tests were promising with a truncated 10-32 countersunk machine screw achieving a 3440 N peak load in lap-shear. Small changes in subsequent iterations lead to peak loads in excess of 5000 N (see Figure 4-25) which is the automotive standard. The limiting factor appeared to be the available bond area which was a factor of the machine screw size. Larger screws were tried, and peak loads increased. The tops of the screws were faced in a lathe to make the drive features shallower so that the driver would not go as deep into the bit and contact weld material. A spacer ensured that downward force was transmitted through the face of the head of the bit and not through the Torx Plus drive features. Drive feature engagement was reduced to less than 1mm, but drivers continued to fail frequently due to the heat and shock of the process. One driver became part of the weld (see Figure 4-26 and Figure 4-27).

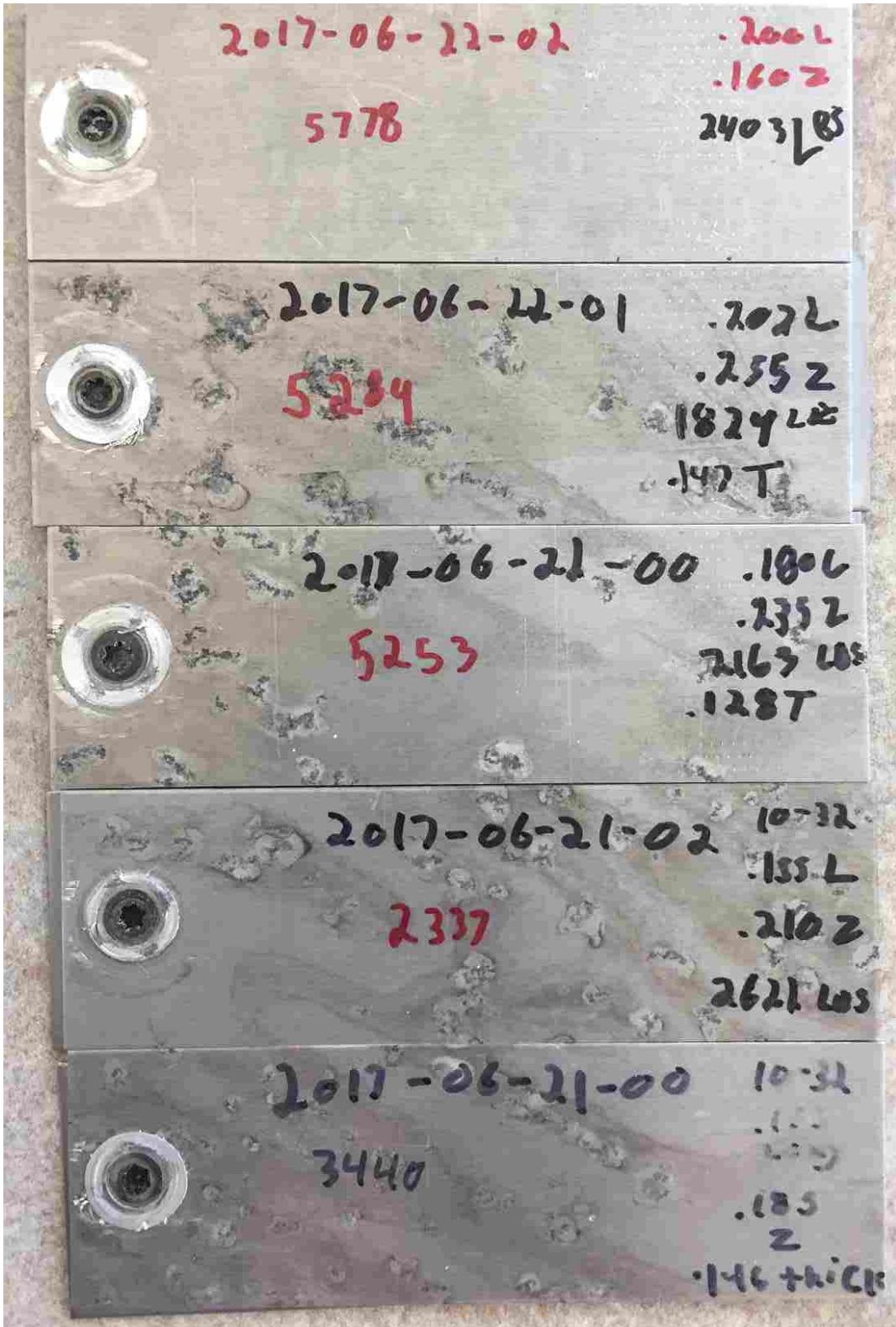


Figure 4-25: Proof-of-Concept Flush Joints Made with Machine Screws



Figure 4-26: Torx Plus Driver Welded to Bit



Figure 4-27: Fracture After Removing Welded Driver from the Bit

Making the drive features shallower reached a point of diminishing returns because the actual drive features of the driver began to fail as engagement was reduced. A different internal drive system was needed to continue with flush bit designs. A survey of current driver technologies lead to inspiration for a new drive feature based on a spanner style tamper-proof screw head which consists of two simple cylindrical pockets. There was a theory among FBJ researchers that a majority of the torque is actual carried by a clutch-like phenomenon and that drive features only really carry torque during the beginning of the weld cycle. Based on this principle, the next drive system used four round pockets that were only .5mm deep to drive the bit. It was a simple design that could be machined quickly.

The first several welds were successful until the feedrate was set too high and the pins driving the bit sheared as the bit formed a bond prematurely. In the next iteration the drive features were moved out radially and enlarged to improve their ability to handle torque. This weakened the bit head so that bits began failing in the head during testing. This is an undesirable failure mode. The four pockets were close enough together that they acted as perforations. To address this, the number of pockets was reduced to three without increasing their size. The frequency of failures went down dramatically, but they still occurred. At this point a more effective cutting system consisting of modified carbide inserts was being used allowing for almost complete flash removal.



Figure 4-28: Bit Head Cracking



Figure 4-29: Severe Fracture of Bit Head



Figure 4-30: Severe Fracture of Bit Head

On a few occasions it was noted that some of the heads developed cracks near the drive features which allowed aluminum to flow into the drive features. To address this, the drive features were reduced in size, a back slope was added, the drive features were moved in radially, and the fillet under the head was increased. All these actions added strength to the head by putting more material back into the head and reducing stress risers. No head failures or cracks have been observed since the change. The back slope in the drive features also aided in locating the drive features when loading the bit onto the driver. It should also be noted that the bits do not have to be sunk flush but can be if strength requirements are still met for a given application.



Figure 4-31: Crack Flowing Aluminum into Drive Feature of Bit

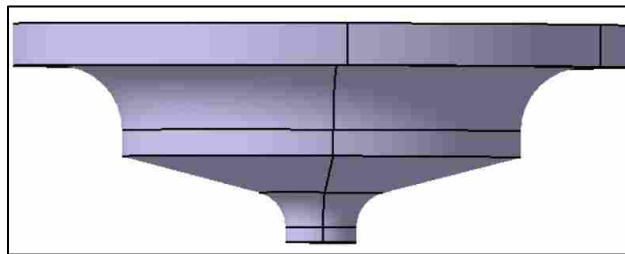


Figure 4-32: Overall Geometries of Current Flush Bit Design

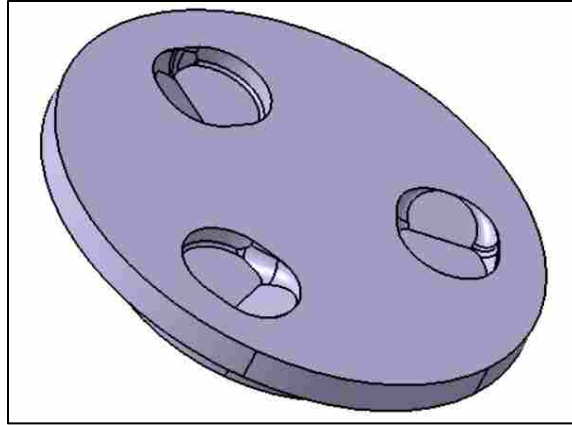


Figure 4-33: Drive Features of Current Bit Design

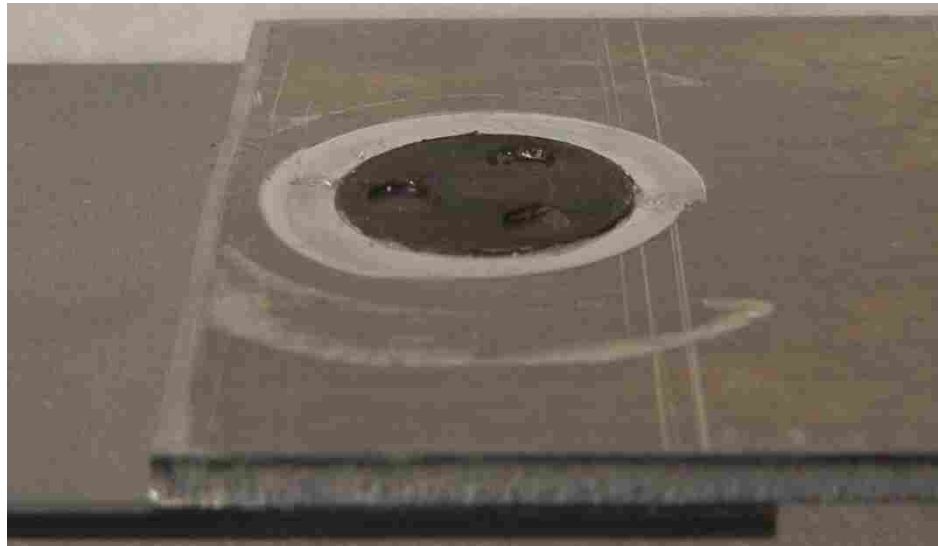


Figure 4-34: Isometric View of Flush FBJ



Figure 4-35: Unpolished Flush FBJ Cross Section

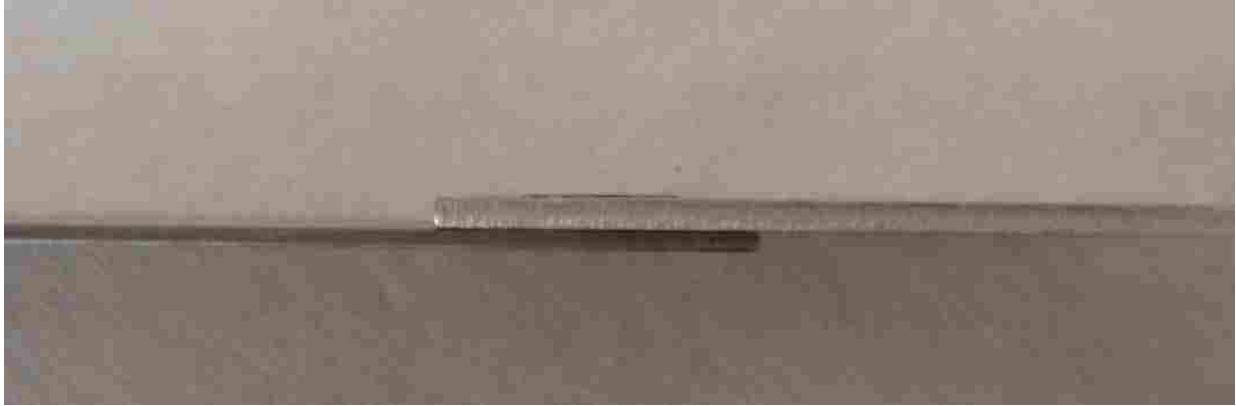


Figure 4-36: Flush FBJ Side View



Figure 4-37: Dies for Pressing Drive Features into Bit Heads

In some cases, some deformations of the drive features in the bit head were observed. These occurrences were mainly during experimental welds where parameters were being pushed beyond the norm and using alternate materials that had different hardness values than the materials covered by this thesis. If the bit is driven too deep, the heat buildup in the bit can be enough to soften the drive features and allow them to smear as can be seen in an extreme case in

Figure 4-38. A more common distortion is slight stretching of the drive features. A more extreme case of this can be seen in figure 4-39. No unusual failure modes during tensile testing have been noticed due to this occasional stretching to date.



Figure 4-38: Severe Smearing of Drive Features During Experiment



Figure 4-39: Less Common Stretching of Drive Features

1-2 kN reductions in peak load in lap-shear were observed, but they were still significantly higher than automotive standards. Peak loads in T-peel were generally in the same range as previous research had achieved. Driving the bits flush cuts into the available aluminum

and weakens the aluminum so a drop in peak load is not unexpected. However, samples still passed requirements and the flush nature of the joint had other desirable qualities.

Table 4-11: T-Peel Peak Loads with Flush FBJ

Sample #	Peak Load (N)
2017-10-04-05	1983
2017-10-05-00	898
2017-10-05-01	2120
2017-10-05-02	2070
2017-10-05-03	2249

Cross sections of lap-shear samples were polished and examined. Further analysis of the grain structures and microhardness will continue after the publication of this thesis. A first examination reveals a thorough heat penetration into the steel layer. The HAZ does not appear to reach the drive features in a normal weld. The bond area appears to be noticeably small than what the diameter of the shank of the bit could potentially provide. Steel flash produced by the friction weld appears to aggressively curl away while some aluminum can be observed still trapped at the interface. It may be that small losses in peak loads with flush bits are attributed to a smaller bond area do to deformation and redirection of the steel flash. Further bit design iterations may be able to either increase the weld bond area or decrease the diameter of the bit to displace less aluminum and provide better hold down strength through greater overlap of the bit head with the aluminum. The steel flash undercuts the aluminum held down by the head and may be reducing peak loads in cross-tension and T-peel. The reduced bit head-aluminum overlap also allows for the bit to tip and peel away from the steel as the aluminum stretches in lap-shear.

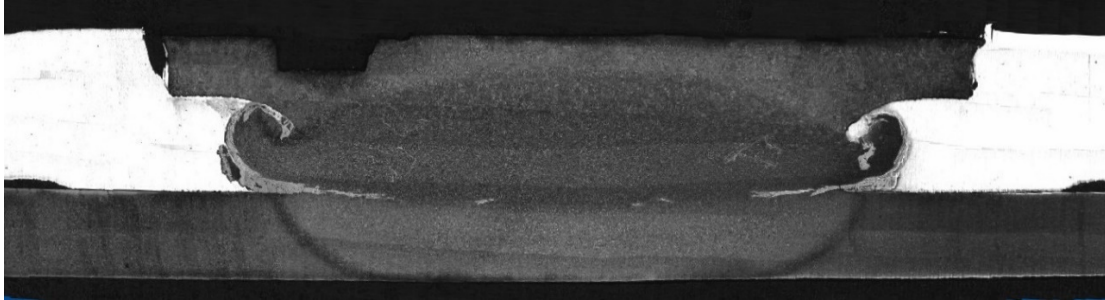


Figure 4-40: Polished Cross Section Microscope View of Flush FBJ Joint

4.6 Surface Finish

As previously mentioned, flash was a major concern. Decreasing the weld depth resulted in reduction in flash. No means of quantifying flash and debris was used. Flash and debris have two suspected causes in the process. The first is the cutting features producing aluminum chips that are supposed to be evacuated by the flutes of the bit, but the chips often get caught and clogged by the ring of flash which relates to the second cause. The ring of flash is likely caused because the shaft of the bit is tapered and the cutting edges on the flutes are not sharp enough to cut effectively so the aluminum is heated by friction and deformed instead of being cut.

In early efforts to reduce flash before the flush bit design was established, an experimental clamp was designed and fabricated to direct the flash and chips away from the aluminum coupon to prevent them from bonding as can be seen in Figure 4-41. However, the deflection in the driver proved to be too much for the bushing in the clamp to handle. The bushings wore out after a few welds because the driver would drift in the same direction each time.

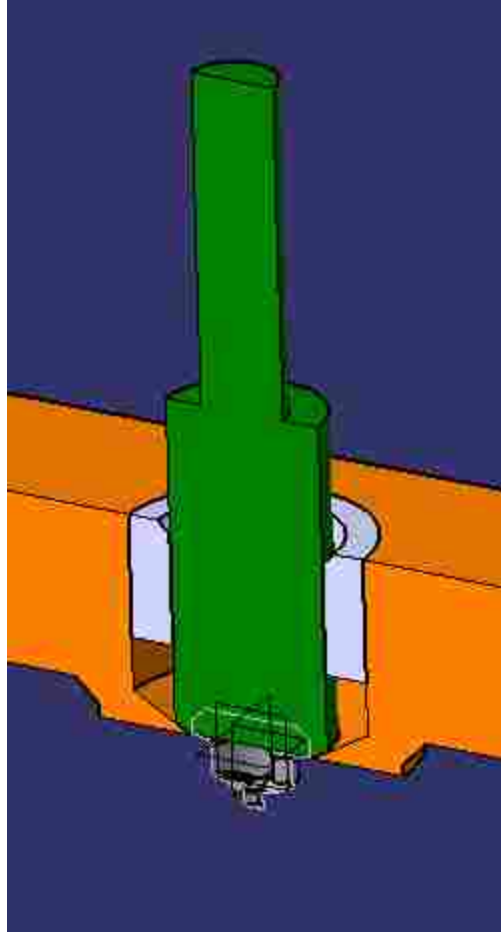


Figure 4-41: Section View of Flash Removal Clamp with Bushing

To improve chip formation and clearance of the chips the Stage 1 parameters were reviewed and found to be less than ideal. The RPM and feedrate were recalculated based on standard drilling calculations to 3703 RPM and 14 IPM. Chip formation seems to have improved, but the flash caused by the taper and dull cutting features still often traps the chips. The rotation and further descent of the bit rubs the chips on the flash effectively bonding the chips to the flash. These new parameters along with the new weld depth resulted in stronger and more consistent joints, however. The improved cutting parameters likely imparted less frictional heat into the aluminum which helps maintain the aluminum's strength, hence the failures were more consistently the steel tearing instead of the aluminum failing for lap-shear.

As part of the efforts to remove aluminum flash from around the head of the FBJ head, a new bit design and driver were investigated. This bit design allows for the head of the bit to be countersunk into the aluminum so that the head is flush with the surrounding aluminum. Drive features were changed to be internal which allowed for carbide cutters to make intimate contact with the aluminum flash generated around the bit head. This resulted in clean, flush joints as shown in Figure 4-34. Because the bit head cuts into the aluminum, some strength is lost, but peak loads to date have approached similar loads as the old design. Weld pressures are greater because of there are no cutting features and because the full volume of the head of the bit must be displaced in the aluminum.

The flash generated by a flush joint can be seen in Figure 4-28. The first drivers equipped with carbide cutters removed significant amounts of flash, but since they were tied to the weld depth, any variation in weld depth could result in left over flash or counterboring around the joint as seen in Figure 4-421.



Figure 4-42: Leftover Flash from Driver with Fixed Cutters

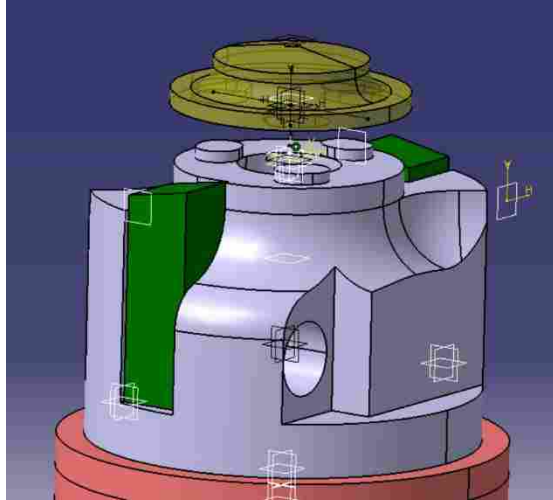


Figure 4-43: Driver with Three Pegs, Fixed Carbide, and Bit



Figure 4-44: 4 Peg Driver Assembly



Figure 4-45: Aluminum Chip Build Up Due to Uneven Cutter Engagement

To address the issue of fixed cutters going too deep or not deep enough, the team designed a floating cutter system that rotated with the driver but was independent axially and could use the clamp as a reference to hold the cutters so that they merely grazed the top of the aluminum while the weld was completed. This meant that the weld depth could be change within a 1.52mm range. This also allowed for the driver to be retracted so that the cutters could then do a final deburring operation without damaging the drive features. In addition, the retractability of the cutters made it possible to pull them out of the way of the feed system.

This driver and cutter system combination have since been used to successfully make hundreds of welds. In one instance the bit came off the driver before engaging in the aluminum and the drive plunged into the aluminum. The driver was made of hardened D2 and sustained no discernable damage. In another occasion a bit was knocked off the driver and jammed between the cutter and clamp block wall, breaking the cutter assembly. Because the keys were oversized, the shank of the driver also cracked. In another instance the bit was also knocked off the driver by the cutters, jamming and breaking the cutters again. The driver survived this

instance. In another situation, due to operator error, the driver did not retract far enough before rotating for the last flash clearing step and instead friction stirred the top of the bit. The driver was still functional afterwards. The drive features on the driver have proven robust. The cutter assembly still needs improvement. A vacuum system for chip removal is already designed and if it had been in use, it would have likely sucked the bit out of the way and prevented the jams.



Figure 4-46: Flush Bit Driver After Several Hundred Welds



Figure 4-47: Flush Bit Driver Full Side View



Figure 4-48: Flush Bit Cutter Assembly

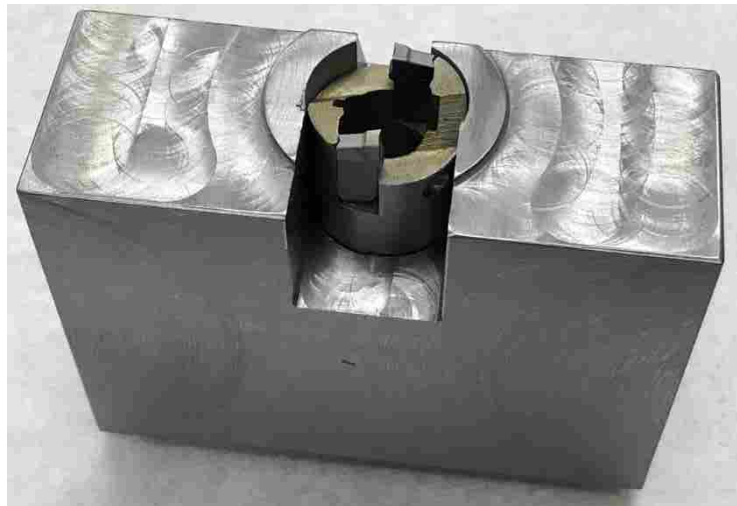


Figure 4-49: Underside View of Cutter Assembly Mounted in Clamp Block



Figure 4-50: Cutter Assembly with Needle Bearing and Thrust Bearing



Figure 4-51: Broken Cutter After Bit Jammed In Clamp Block

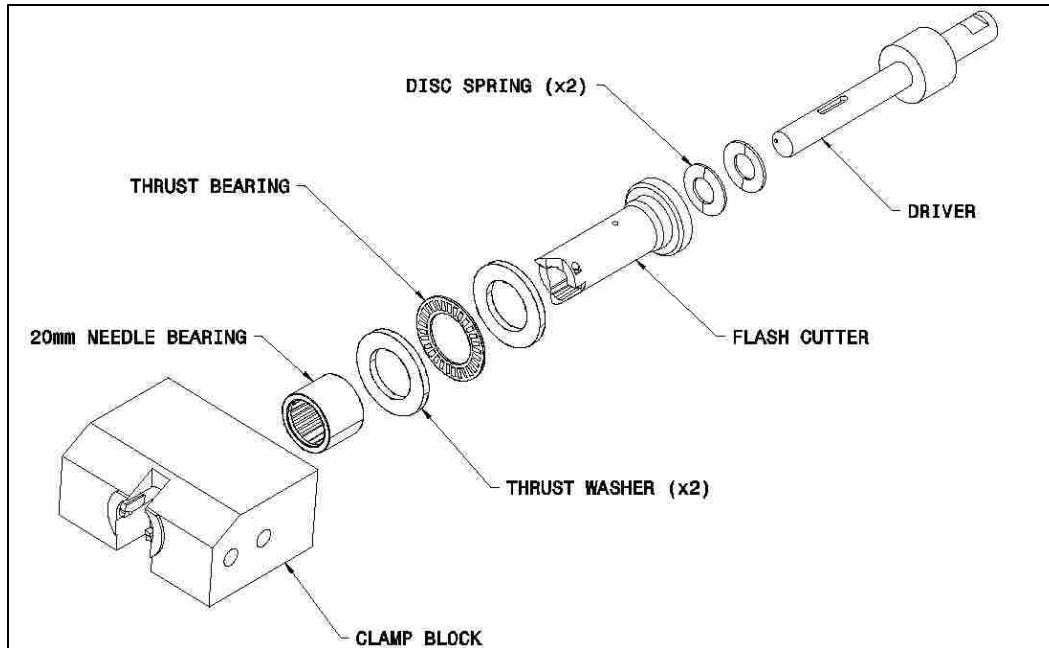


Figure 4-52: Full Clamp-Cutter-Driver Assembly

4.7 Corrosion

Corrosion testing had been performed to some degree by previous FBJ research. A second round of corrosion tests were completed by Honda on specimens using both adhesives and FBJ joints together. This batch of samples used the older style of bit. Previous issues of corrosion initiation where edges of the two different coupons lined up were addressed in this test by making the steel coupons 10mm wider. Results improved over the previous corrosion testing, however, the specimens did not meet the required strength retention. The specimens were required to retain at least 90% of their peak load after testing, but they ended up holding only 50%. The aluminum appears to have delaminated below the adhesive while the adhesive stayed intact. The FBJ joints broke at close to their full strengths. The aluminum delamination was the main premature failure. Because of this, Honda tasked the FBJ team with producing a third corrosion submission. The submission included two adhesives and two bit designs including the

flush bit design. It was hoped that the flush joints will be easier to apply an anti-corrosion layer to and that the smooth surface around the joint would minimize corrosion antennas. Due to limited capacity and time, not all the requested samples could be produced on time, but enough were provided to Honda to meet their needs. The testing is still ongoing, and results are pending.



Figure 4-53: A Portion of the Samples Produced for the Corrosion Submission

5 CONCLUSIONS AND RECOMMENDATIONS

5.1 Conclusions

Friction Bit Joining has shown promise as a viable means for joining UHSS to aluminum. It has successfully joined aluminum to a variety of UHSS. This unique ability to bond lightweight materials to UHSS will be critical to the automotive industry's efforts to achieve CAFE fuel economy standards by 2025. Six hypotheses were tested in this research to make FBJ production ready for the automotive industry.

The purpose of this research was to bring FBJ technology closer to a point where it is ready for an automated production environment. To achieve these goals six hypotheses were investigated and are concluded as follows:

1. Machine parameters, bit design and machine design can be empirically optimized for strength and reliability in T-peel, lap shear, and cross tension though each test may require a different combination for optimization.

This hypothesis is not rejected. Through a Design of Experiments, it was found that there was not a universal set of machine parameters to optimize peak load in all three joint configurations. The effects of the machine parameters are such that optimizing for lap-shear, which is the easiest test to perform, does not optimize for T-peel which is the most severe test.

Future testing will benefit from knowing that parameter optimization should be focused exclusively on T-peel since the other configurations pass their requirements so easily.

2. The strength of consecutive FBJ welds parallel to the bonded edge on the same work piece are additive regardless of their spacing and whether the welds are made in combination with an adhesive.

This hypothesis is not rejected. When multiple FBJ joints were made on the same coupon assembly, regardless of the spacing and number of welds, peak loads were approximately additive assuming all the welds were “good.” “Bad” welds would fail prematurely and send their load to the surrounding joints causing them to fail prematurely. However, it should be noted that it could not be determined for certain that “bad” welds were not caused by the multi-weld scenario. Most samples did sustain a peak load proportional to the number of FBJ welds though, so it is likely they are mostly additive in nature. Load paths as measured by DIC were predictably concentrated around the edge side of the bit.

3. Cutting features on FBJ bits are not always beneficial to FBJ of GADP 1180 to AA 7085-T76 as compared to a bit with no cutting features.

This hypothesis is not rejected. By testing bits with no cutting features and ultimately moving towards a design with not only no cutting features, but also a significantly larger volume of aluminum to be displaced, it was proven that the benefits of cutting features are not always needed for joining GADP 1180 to AA 7085-T76. The cutting features are useful for piercing thicker or harder material combinations but can be left out for this combination with little to no negative effects on peak loads.

4. Surface finish can be improved through machine parameter, bit design and tool design optimization.

This hypothesis is not rejected. By creating a floating cutter system that grazes the surface of the aluminum top layer, the FBJ team was able to create smooth, flush joints which Honda approved of. This surface finish is important for several reasons: it reduces hazards to factory workers, it improves cosmetics, it improves adhesion of anti-corrosion coatings and paint, and it eliminates corrosion antennas.

5. In a FBJ joint of GADP 1180 to AA 7085-T76 the aluminum will fail first in low load, high cycle fatigue testing, but the steel will fail first in high load, low cycle fatigue testing.

This hypothesis is not rejected. Lap-shear joints were cycled at three different ranges of tensile loads until failure. In almost all cases, the aluminum failed first in low load, high cycle scenarios presumably because it has no fatigue limit and therefore weakens with each cycle while the load is too small to reach the steel's fatigue limit. The joint itself survived all the tests. This highlights the important of material choices when designing structures for fatigue.

6. FBJ joints of GADP 1180 to AA 7085-T76 can be made to withstand corrosion testing if protected by a corrosion inhibiting coating after being joined.

This hypothesis cannot yet be evaluated fully as corrosion test results are still pending. Generally, there have been marked improvements in the ability for these joints to maintain their strength after extended periods of time in a corrosion chamber, but they have not yet met Honda's requirements. The new, flush bit design is still hoped to resolve this issue.

5.2 Recommendations

Areas of further research would include robustness of the whole system in an automated production setting with a feed system, developing a more robust method for securing the bit to the driver instead of a heat sensitive magnet, integration of a feedback loop such as a vision system to avoid damage to the system, final selection of a production method, coatings to protect the bit from corrosion, and application of flush bits with other material combinations. More testing of the robustness of flush FBJ may lead to improvements in peak loads. Additionally, flush FBJ welds should be tested in fatigue because they may have different results since they displace more aluminum. Also, the process may benefit from moving towards a load control system instead of a Z displacement control.

REFERENCES

- Abe, Y., T. Kato, and K. Mori. "Self-Piercing Riveting of High Tensile Strength Steel and Aluminium Alloy Sheets using Conventional Rivet and Die." *Journal Material Processing Technology*, 2009: 3914-3922.
- Albrecht, S., M. Baumann, C. P. Brandstetter, R. Horn, H. Krieg, M. Fischer, and R. Ilg. "Environmental Aspects of Lightweight Construction in Mobility and Manufacturing." *Green Design, Materials and Manufacturing Processes* (2013): 185.
- Bates, P. D., Stewart, M. D., Desitter, A., Anderson, M. G., Renaud, J. P., and Smith, J. A. (2000). "Numerical Simulation of Floodplain Hydrology." *Water Resources Research*, 36(9), 2517-2529.
- Bedient, P. B. and Huber, W. C. (1988). *Hydrology and Floodplain Analysis*, Addison-Wesley
- Deptula, L. and Noah, A., "Estimating the Cost Impact of Lightweighting Automotive Closures," SAE Technical Paper 2015-01-0581, 2015, doi:10.4271/2015-010581.
- Groche, P., S. Wohletz, M. Brenneis, C. Pabst, and F. Resch, Joining by Forming—A Review on Joint Mechanisms, Applications and Future Trends, *J. Mater. Process. Technol.*, 2014, 214, p 1062–1093
- Huang, T., Y.s. Sato, H. Kokawa, M.p. Miles, K. Kohkonen, B. Siemssen, R.j. Steel, and S. Packer. "Microstructural Evolution of DP980 Steel during Friction Bit Joining." *Metall and Mat Trans a Metallurgical and Materials Transactions A* 40.12 (2009):2994-3000.
- Kuziak, R., R. Kawalla, and S. Waengler. "Advanced High Strength Steels for Automotive Industry." *Archives of Civil and Mechanical Engineering* 8.2 (2008):103-117.
- Lai, M., R. Brun, Latest Developments in Sheet Metal Forming Technology and Materials for Automotive Application: The Use of Ultra High Strength Steels at Fiat to Reach Weight Reduction at Sustainable Costs, *Key Eng. Mater.*, 2007, 344, p 1–8
- Matlock, D. K., and J. G. Speer. "Third Generation of AHSS: Microstructure Design Concepts." *Microstructure and Texture in Steels*. Springer London, 2009. 185-205.
- Miles, M., S. T. Hong, C. Woodward, Y. H. Jeong. "Spot Welding of Aluminum and Cast Iron by Friction Bit Joining." *International Journal of Precision Engineering and Manufacturing* 14.6 (2013): 1003-1006.

- Miles, M. P., K. Kohkonen, S. Packer, R. Steel, B. Siemssen, and Y. S. Sato. "Solid State Spot Joining of Sheet Materials using Consumable Bit." *Science and Technology of Welding & Joining*, 2009: 72-77.
- Miles, M. P., et al. "Spot Joining Of AA 5754 And High Strength Steel Sheets By Consumable Bit." *Science & Technology Of Welding & Joining* 15.4 (2010): 325-330. Academic Search Premier. Web. 31 Jan. 2017.
- Pouranvari, M., and S. P. H. Marashi. "Critical Review of Automotive Steels Spot Welding: Process, Structure and Properties." *Science and Technology of Welding and Joining* 18.5 (2013): 361-403.
- Qiu, R., C. Iwamoto, S. Satonaka. "Interfacial microstructure and strength of steel/aluminum alloy joints welded by resistance spot welding with cover plate," *J. Mater. Proc. Technol.* 209 (2009) 4186-4193.
- Rhodes, C. G., M. W. Mahoney, W. H. Bingel, R. A. Spurling, and C. C. Bampton. "Effects of Friction Stir Welding On Microstructure of 7075 Aluminum." *Scripta Materialia* 36.1 (1997): 69-75.
- Schneider, J., and R. Radzilowski. "Welding of Very Dissimilar Materials (Fe-Al)." *Jom* 66.10 (2014): 2123-129. Web. 30 Jan. 2017.
- Squires, L. P. "Friction Bit Joining of Dissimilar Combinations of Advanced High-Strength Steel and Aluminum Alloys." (2014). All Theses and Dissertations. Paper 4104.